bioRxiv preprint doi: https://doi.org/10.1101/2021.03.23.436585; this version posted March 23, 2021. The copyright holder for this preprint (which was not certified by peer review) is the author/funder, who has granted bioRxiv a license to display the preprint in perpetuity. It is made available under aCC-BY 4.0 International license.

Prostaglandin E_2 induction by cytosolic *Listeria monocytogenes* in phagocytes is necessary for optimal T-cell priming

Courtney E. McDougal[1], Zachary T. Morrow[1], Seonyoung Kim[2], Drake Carter[2], David M. Stevenson[3], Daniel Amador-Noguez[3], Mark J. Miller[2], John-Demian Sauer[1,*]

1. Department of Medical Microbiology and Immunology, University of Wisconsin-Madison, Madison, Wisconsin, United States of America
2. Department of Internal Medicine, Division of Infectious Diseases, Washington University School of Medicine, St. Louis, Missouri, United States of America
3. Department of Bacteriology, University of Wisconsin-Madison, Madison, Wisconsin, United States of America

[*] Corresponding Author
Email: sauer3@wisc.edu (JDS)

bioRxiv preprint doi: https://doi.org/10.1101/2021.03.23.436585; this version posted March 23, 2021. The copyright holder for this preprint (which was not certified by peer review) is the author/funder, who has granted bioRxiv a license to display the preprint in perpetuity. It is made available under aCC-BY 4.0 International license.

Abstract

Listeria monocytogenes is an intracellular bacterium that elicits robust $CD8^+$ T-cell responses. Despite the ongoing development of *L. monocytogenes*-based platforms as cancer vaccines, our understanding of how *L. monocytogenes* drives robust $CD8^+$ T-cell responses remains incomplete. One overarching hypothesis is that activation of cytosolic innate pathways is critical for immunity, as strains of *L. monocytogenes* that are unable to access the cytosol fail to elicit robust $CD8^+$ T-cell responses and in fact inhibit optimal T-cell priming. Counterintuitively, however, activation of known cytosolic pathways, such as the inflammasome and type I IFN, lead to impaired immunity. Here, we describe a cytosol-dependent response that is critical for immunity to *L. monocytogenes*, namely production of prostaglandin E_2 (PGE_2) downstream of cyclooxygenase-2 (COX-2). Vacuole-constrained *L. monocytogenes* elicit reduced PGE_2 production compared to wild-type strains in macrophages and dendritic cells *ex vivo*. *In vivo,* infection with wild-type *L. monocytogenes* leads to 10-fold increases in PGE_2 production early during infection whereas vacuole-constrained strains fail to induce PGE_2 over mock-immunized controls. Mice deficient in COX-2 specifically in $Lyz2^+$ or $CD11c^+$ cells produce less PGE_2, suggesting these cell subsets contribute to PGE_2 levels *in vivo,* while depletion of phagocytes with clodronate abolishes PGE_2 production completely. Taken together, this work identifies the first known cytosol-dependent innate immune response critical for generating $CD8^+$ T-cell responses to *L. monocytogenes,* suggesting that one reason cytosolic access is required to prime $CD8^+$ T-cell responses may be due to induction of PGE_2.

bioRxiv preprint doi: https://doi.org/10.1101/2021.03.23.436585; this version posted March 23, 2021. The copyright holder for this preprint (which was not certified by peer review) is the author/funder, who has granted bioRxiv a license to display the preprint in perpetuity. It is made available under aCC-BY 4.0 International license.

Author summary

L. monocytogenes is an intracellular bacterial pathogen that generates robust cell-mediated immune responses. Due to this robust induction, *L. monocytogenes* is used as both a model to understand how CD8+ T-cells are primed, as well as a platform for cancer immunotherapy vaccines. *L. monocytogenes* must enter the cytosol of an infected host cell to stimulate robust T-cell responses, however, which cytosolic innate pathway(s) contribute to T-cell priming remains unclear. Here, we define COX-2 dependent PGE_2 production as the first cytosol-dependent innate immune response critical for immunity to *L. monocytogenes*. We found that *ex vivo* PGE_2 production by macrophages and dendritic cells is partially dependent on cytosolic access, as vacuole-constrained strains of *L. monocytogenes* elicit reduced PGE_2. *In vivo,* cytosolic access is essential for PGE_2 production. *L. monocytogenes* elicits a 10-fold increase in PGE_2 production, whereas strains of *L. monocytogenes* that cannot access the cytosol fail to elicit PGE_2 compared to mock immunized mice. Furthermore, $CD11c^+$ and $Lyz2^+$ cells contribute to PGE_2 production *in vivo*, as mice deficient in COX-2 in these cell subsets have impaired PGE_2 production. Taken together, our work identifies the first known cytosol-dependent pathway that is critical for generating immunity to *L. monocytogenes*.

bioRxiv preprint doi: https://doi.org/10.1101/2021.03.23.436585; this version posted March 23, 2021. The copyright holder for this preprint (which was not certified by peer review) is the author/funder, who has granted bioRxiv a license to display the preprint in perpetuity. It is made available under aCC-BY 4.0 International license.

Introduction

Listeria monocytogenes is a Gram-positive, intracellular pathogen that elicits robust $CD8^+$ T-cell responses. Due to this robust response, *L. monocytogenes* has been used for decades as a model to understand how $CD8^+$ T-cell responses are primed[1]. Understanding these responses has become more pressing recently as *Listeria*-based platforms aiming to drive $CD8^+$ T-cell responses are in use as cancer immunotherapies[2]. Initial work showed that critical signals promoting *Listeria*-stimulated T-cell responses are provided acutely, as bacterial clearance with antibiotics as early as 24 hours-post infection has minimal impact on the kinetics of $CD8^+$ T-cell responses[3]. This work highlights the role of early signals in informing *Listeria*-stimulated cell mediated adaptive responses.

One early signal impacting T-cell responses is the inflammatory environment induced during infection. The importance of the inflammatory milieu on priming T-cell responses has been solidified by multiple groups using antigen-pulsed, matured dendritic cells in combination with non-antigen expressing *L. monocytogenes* as an inflammatory boost[4,5]. These studies enable discrimination between antigen presentation and inflammation and demonstrate that wild-type *L. monocytogenes* provides an optimal inflammatory milieu to drive T-cell priming[4,5]. The inflammatory boost provided through wild-type *L. monocytogenes* infection led to increased T-cell responses, whereas use of strains that specifically alter the inflammatory milieu led to suboptimal responses[4,5]. *L. monocytogenes* activates a number of innate pathways that contribute to the inflammatory milieu. In particular, multiple groups have focused on the role of various cytosolic innate immune pathways, as previous research demonstrated the necessity of cytosolic access in priming cell-mediated immunity[6–8]. *L. monocytogenes* utilizes a cytolysin, listeriolysin O (LLO), to escape from phagosomes directly into the cytosol and LLO-deficient

bioRxiv preprint doi: https://doi.org/10.1101/2021.03.23.436585; this version posted March 23, 2021. The copyright holder for this preprint (which was not certified by peer review) is the author/funder, who has granted bioRxiv a license to display the preprint in perpetuity. It is made available under aCC-BY 4.0 International license.

mutants that are unable to access the cytosol inhibit T-cell priming and generate tolerizing immune responses[9,10]. Despite the importance of cytosolic access for priming T-cell responses, multiple cytosol-dependent innate pathways are counterintuitively detrimental to immunity including STING-dependent type I interferon[11,12] as well as inflammasome activation[4,13]. We recently identified an alternative innate pathway, production of the eicosanoid prostaglandin E_2 (PGE_2), as important for immunity as mice deficient in PGE_2 have impaired acute and protective T-cell responses to *L. monocytogenes*[14]. Whether PGE_2 production is dependent on cytosolic access of *L. monocytogenes* remains unknown as is which cells produce PGE_2 in response to *L. monocytogenes* infection.

Eicosanoids are lipid mediators of inflammation that have potent biological functions. A major subset of these lipids, including PGE_2, are derived from arachidonic acid[15]. During inflammation, arachidonic acid is liberated from the membrane by the cytosolic phospholipase A2 (cPLA2) and then further metabolized by a number of enzymes including the P450 epoxygenase, lipoxygenases, and cyclooxygenases (COXs)[15]. During infection, PGE_2 is produced downstream of COX enzymes, particularly downstream of cyclooxygenase-2 (COX-2)[16]. COX-2 is induced during inflammation and functions to reduce arachidonic acid to prostaglandin H_2 (PGH_2)[17,18]. PGH_2 is further metabolized into different prostaglandins by terminal prostaglandin synthases. Coupling of COX enzymes with prostaglandin synthases ultimately dictates which prostaglandin will be produced[17,18]. PGE_2 specifically is produced by three different terminal synthases, the cytosolic prostaglandin E synthase (cPGES) and microsomal prostaglandin E synthases-1 and -2 (mPGES-1 and mPGES-2)[16,19]. Of these synthases, mPGES-1 is inducible and associated with infection due to its role in inflammatory responses[16,19]. For example, mice deficient in mPGES-1 have reduced febrile and pain

bioRxiv preprint doi: https://doi.org/10.1101/2021.03.23.436585; this version posted March 23, 2021. The copyright holder for this preprint (which was not certified by peer review) is the author/funder, who has granted bioRxiv a license to display the preprint in perpetuity. It is made available under aCC-BY 4.0 International license.

responses[16,19]. Previously, we showed that *L. monocytogenes* infection of mice deficient in mPGES-1 or use of a COX-2-specific inhibitor leads to impaired T-cell responses that could be rescued by exogenous dosing of PGE_2[14]. Together, these data suggest that production of PGE_2 downstream of COX-2 and mPGES-1 is critical for immunity.

During *L. monocytogenes* infection, the cell types responsible for producing PGE_2 remain unclear. *L. monocytogenes* is initially captured by a wide range of phagocytic antigen presenting cells (APCs) in the marginal zone of the spleen[20]. Initially, *L. monocytogenes* highly infects multiple macrophage subsets, including $MOMA^+$ metallophilic and $MARCO^+$ marginal zone macrophages[20]. Later, *L. monocytogenes* infection transitions to splenic $CD11c^+$ and $CD11b^+$ cells in the white pulp[20]. Importantly, PGE_2 is produced at high amounts early in the immune response, starting at four hours post immunization and peaking at twelve hours, early timepoints during which macrophages and dendritic cells are heavily infected[14]. Furthermore, one previous study demonstrated that peritoneal macrophages are capable of producing PGE_2 after *ex vivo* infection with *L. monocytogenes*[21]. Further analysis is required to elucidate whether macrophages and dendritic cells similarly produce PGE_2 *in vivo.*

Here, we demonstrated *ex vivo* that macrophages and dendritic cells produce PGE_2 in response to *L. monocytogenes* infection. Importantly, induction of PGE_2 *ex vivo* was partially dependent on cytosolic access, as infection of bone marrow-derived macrophages or dendritic cells with vacuole-constrained *L. monocytogenes* led to reduced PGE_2 compared to wild-type strains. In contrast, *in vivo* PGE_2 production requires cytosolic access, as infection with LLO-deficient *L. monocytogenes* led to a complete lack of PGE_2 induction, similar to mock-immunized levels. $Lyz2^+$ and $CD11c^+$ cells contribute to PGE_2 production *in vivo,* as deletion of COX-2 selectively in these subsets led to reduced splenic PGE_2 levels. However, these subsets

bioRxiv preprint doi: https://doi.org/10.1101/2021.03.23.436585; this version posted March 23, 2021. The copyright holder for this preprint (which was not certified by peer review) is the author/funder, who has granted bioRxiv a license to display the preprint in perpetuity. It is made available under aCC-BY 4.0 International license.

122 are not solely responsible for production as a small amount of PGE_2 remains and this remaining
123 PGE_2 is sufficient to facilitate optimal T-cell priming. Use of phagocyte-depleting clodronate
124 treatment completely eliminated PGE_2 production to mock-immunized levels. Taken together,
125 this work identifies, for the first time, a cytosolic-dependent pathway critical for inducing
126 immunity to *L. monocytogenes.* We show that phagocytes, particularly macrophages and
127 dendritic cells, produce PGE_2 in a cytosol-dependent manner.

bioRxiv preprint doi: https://doi.org/10.1101/2021.03.23.436585; this version posted March 23, 2021. The copyright holder for this preprint (which was not certified by peer review) is the author/funder, who has granted bioRxiv a license to display the preprint in perpetuity. It is made available under aCC-BY 4.0 International license.

Results

Unprimed macrophages and dendritic cells upregulate PGE_2-synthesizing enzymes in response to cytosolic *L. monocytogenes*

We previously demonstrated that immunization of mice with *L. monocytogenes* induces production of PGE_2, starting at four hours post infection and peaking at twelve hours, and that this transient PGE_2 production is necessary for optimal T-cell priming[14]. During infection, *L. monocytogenes* infects multiple phagocytic cell populations in the spleen, the majority of which are macrophage and dendritic cell subsets[20]. Initially, *L. monocytogenes* localizes to multiple macrophage subsets[20] and by twelve hours after infection, $CD11c^+$ dendritic cells comprise the largest subset of *L. monocytogenes* infected cells[20]. We hypothesized that macrophages and dendritic cells were the subsets producing PGE_2 due these cells being the predominantly infected cell subsets at these early timepoints post immunization. To determine if *L. monocytogenes* infection induces the genes necessary for PGE_2 production, we first measured expression of *Pla2g4a* mRNA (encoding cPLA2), a phospholipase that releases arachidonic acid from the cell membrane[15], in bone marrow derived macrophages (BMDMs) and bone marrow derived dendritic cells (BMDCs). BMDMs and BMDCs were infected with *L. monocytogenes* and mRNA was harvested six hours later. We found that cPLA2 expression did not change during *L. monocytogenes* infection (S1 Fig). This result was not surprising, as much of cPLA2 activity is modulated by calcium influx and MAPK phosphorylation rather than transcriptional changes[22]. We next measured mRNA expression of *Ptgs2* (encoding COX-2) and *Ptges* (encoding mPGES-1), encoding enzymes involved in the next steps of PGE_2 synthesis[16,19]. In both BMDMs and BMDCs, infection with wild-type *L. monocytogenes* led to an increase in *Ptgs2* expression and, to a lower extent, *Ptges*, suggesting that macrophages and dendritic cells

bioRxiv preprint doi: https://doi.org/10.1101/2021.03.23.436585; this version posted March 23, 2021. The copyright holder for this preprint (which was not certified by peer review) is the author/funder, who has granted bioRxiv a license to display the preprint in perpetuity. It is made available under aCC-BY 4.0 International license.

could be capable of synthesizing PGE_2 (Fig 1A-B). Given that PGE_2 is necessary for optimal T-cell priming and that immunizing mice with a strain of *L. monocytogenes* that cannot access the cytosol leads to reduced T-cell effector function[9,10], we hypothesized that impaired T-cell responses to vacuole constrained bacteria may be due to reduced expression of PGE_2-synthesizing enzymes and ultimately decreased production of PGE_2. To test this hypothesis, we infected BMDMs and BMDCs with a vacuole-constrained strain of *L. monocytogenes* (Δ*hly*, a mutant lacking the pore-forming protein LLO) and assessed expression of *Ptges* and *Ptgs2* mRNA. Consistent with this hypothesis, infection with this strain led to reduced *Ptgs2* expression in BMDMs and BMDCs, suggesting that cytosolic access is required for optimal expression of *Ptgs2* (Fig 1A). Interestingly, infection with Δ*hly L. monocytogenes* led to similar levels of *Ptges* expression in both BMDMs and BMDCs (Fig 1B). Taken together, these results suggest that cytosolic access increases *Ptgs2* expression in BMDMs and BMDCs, whereas *Ptges* expression is induced independently of cytosolic access. Additionally, as controls we assessed expression of *Ifnb1* (encoding IFN-β) and *Il1b* (encoding IL-1β) in BMDMs and BMDCs. As expected, *Ifnb1* was expressed only during infection with cytosolic, wild-type *L. monocytogenes* in both cell subsets (S1 Fig), where *Il1b* was induced by TLR signaling during infection with both wild-type and Δ*hly L. monocytogenes* infection (S1 Fig).

Given that *Ptgs2* expression was higher during infection with wild-type compared to Δ*hly L. monocytogenes*, we next assessed whether the increased transcript in wild-type infection led to increased COX-2 protein expression. To assess the role of cytosolic access on COX-2 protein levels, we infected BMDMs or BMDCs with wild-type or Δ*hly L. monocytogenes* and assessed COX-2 protein expression six hours later by western blot. In BMDMs, interestingly, infection

bioRxiv preprint doi: https://doi.org/10.1101/2021.03.23.436585; this version posted March 23, 2021. The copyright holder for this preprint (which was not certified by peer review) is the author/funder, who has granted bioRxiv a license to display the preprint in perpetuity. It is made available under aCC-BY 4.0 International license.

with either strain of *L. monocytogenes* led to increased COX-2 protein expression (Fig 1C). In BMDCs, alternatively, Δ*hly L. monocytogenes* induced lower levels of COX-2 protein (Fig 1C). This suggests that cytosolic access is required for robust induction of COX-2 protein expression in BMDCs.

Infection of BMDMs and BMDCs with wild-type *L. monocytogenes* led to expression of the genes necessary for PGE_2 production (Fig 1A-C). To assess whether these cells could utilize these enzymes to produce PGE_2, we assessed PGE_2 production in culture supernatant by mass spectrometry. Surprisingly, supernatant from both BMDMs and BMDCs had no detectable PGE_2 compared to PBS-treated controls, both during infection with wild-type or Δ*hly L. monocytogenes* (Fig 1D). This suggests that either enzyme expression was not high enough to induce detectable PGE_2, or there may be additional post transcriptional modifications required for enzyme activity. Analysis of PGE_2 from BMDMs or BMDCs deficient in COX-2 had no detectable PGE_2, as expected (Fig 1D).

Primed BMDMs and BMDMs produce PGE_2 during cytosolic *L. monocytogenes* infection

The lack of PGE_2 produced by BMDMs and BMDCs in response to *L. monocytogenes* infection was surprising given the upregulation of *Ptgs2* and *Ptges* transcript. Other innate pathways, such as the inflammasome, require a priming step in order to induce optimal activation. We hypothesized that macrophages may similarly require additional stimulation in order to produce PGE_2. To test this hypothesis, we treated BMDMs and BMDCs overnight with the TLR2 agonist PAM3CSK4 (PAM) before infection with wild-type and Δ*hly L. monocytogenes* and again analyzed transcript expression. PAM alone induced a small amount of expression of *Ptgs2*

bioRxiv preprint doi: https://doi.org/10.1101/2021.03.23.436585; this version posted March 23, 2021. The copyright holder for this preprint (which was not certified by peer review) is the author/funder, who has granted bioRxiv a license to display the preprint in perpetuity. It is made available under aCC-BY 4.0 International license.

197 expression in both BMDMs and BMDCs (Fig 1A). Infection with wild-type *L. monocytogenes*
198 led to a significant increase in expression that was less robust in Δ*hly L. monocytogenes*-infected
199 cells, similar to the effect seen in unprimed cells (Fig 1A). *Ptges* expression, alternatively, had a
200 larger increase in transcript expression during PAM-priming, both during wild-type and Δ*hly L.*
201 *monocytogenes* infection of BMDMs and BMDCs (Fig 1B). Furthermore, PAM treatment alone
202 induced expression of *Ptges* similar to that induced during infection in BMDMs (Fig 1B). Taken
203 together, these data suggest that cytosolic access accentuates expression of *Ptgs2*, where TLR
204 signaling alone is sufficient to induce *Ptges* expression. We also assessed expression of *Pla2g4a*
205 in TLR-primed BMDMs and BMDCs and, similar to unprimed cells, saw no changes in
206 expression (S1 Fig). Additionally, *Ifnb1* transcript was again induced during cytosolic infection,
207 where *Il1b* expression was induced during PAM-treatment alone, as well as during infection with
208 wild-type or Δ*hly L. monocytogenes* (S1 Fig).
209
210 As *Ptgs2* expression was also dependent on cytosolic access in primed BMDMs and BMDCs, we
211 next assessed expression of COX-2 protein in primed cells infected with wild-type or Δ*hly L.*
212 *monocytogenes* by western blot. Similar to unprimed cells, BMDMs had similar levels of COX-2
213 protein during infection with wild-type or Δ*hly L. monocytogenes* (Fig 1C). In BMDCs,
214 alternatively, COX-2 protein expression was reduced during infection with Δ*hly L.*
215 *monocytogenes* compared to wild-type infection (Fig 1C), again suggesting that COX-2 protein
216 expression in BMDCs is potentiated by cytosolic access.
217
218 We hypothesized that priming BMDMs and BMDCs with PAM would stimulate the cells to
219 produce PGE_2 during infection with wild-type *L. monocytogenes*. To test this hypothesis, we

bioRxiv preprint doi: https://doi.org/10.1101/2021.03.23.436585; this version posted March 23, 2021. The copyright holder for this preprint (which was not certified by peer review) is the author/funder, who has granted bioRxiv a license to display the preprint in perpetuity. It is made available under aCC-BY 4.0 International license.

assessed production of PGE_2 in the supernatant of primed BMDMs and BMDCs by mass spectrometry. BMDMs and BMDCs were treated overnight with PAM before infection with wild-type and Δ*hly L. monocytogenes.* Six hours post-infection, cell supernatant was assessed for PGE_2. In contrast to unprimed BMDM and BMDCs, wild-type infection of primed cells led to a significant increase in PGE_2 production compared to PBS-treated controls (Fig 1D). Previous data showed *L. monocytogenes*-stimulated PGE_2 production in peritoneal macrophages[21,23]. Our data suggest that priming BMDMs prior to infection induces the cells to behave more like tissue resident macrophages in respect to PGE_2 production. Furthermore, the ability of BMDMs to produce PGE_2 provides a tool to efficiently study PGE_2 synthesis in macrophages during infection. Importantly, maximal PGE_2 production in primed BMDM and BMDCs was dependent on cytosolic access, as infection with Δ*hly L. monocytogenes* led to significantly reduced PGE_2 levels (Fig 1D). PAM-primed COX-2 deficient BMDMs and BMDCs again led to no PGE_2 production, solidifying the necessity of COX-2 activity in PGE_2 production (Fig 1D).

Additionally, we also sought to understand whether PGE_2 specifically was being induced, or if there was a more broad increase eicosanoid production. To test the hypothesis that *L. monocytogenes* induces production of other eicosanoids, we analyzed production of prostaglandin D_2 (PGD_2), thromboxane B_2 (TXB_2), and leukotriene B_4 (LTB_4). However, we saw no changes production of these eicosanoids by wild-type *L. monocytogenes* (S2 Fig). This interesting observation suggests that macrophages and dendritic cells preferentially induce PGE_2 in response to infection with cytosolic *L. monocytogenes*.

Cytosolic access is required for PGE_2 production *in vivo*

bioRxiv preprint doi: https://doi.org/10.1101/2021.03.23.436585; this version posted March 23, 2021. The copyright holder for this preprint (which was not certified by peer review) is the author/funder, who has granted bioRxiv a license to display the preprint in perpetuity. It is made available under aCC-BY 4.0 International license.

Production of PGE_2 by TLR-primed BMDMs and BMDCs *ex vivo* is potentiated by cytosolic access. To assess whether *L. monocytogenes* induces PGE_2 in a cytosol-dependent manner *in vivo*, we infected mice intravenously with wild-type and Δ*hly L. monocytogenes* and assessed PGE_2 levels in the spleen twelve hours post-infection, previously defined as the peak PGE_2 response to infection[14]. Wild-type *L. monocytogenes* led to an eight-fold increase in PGE_2 (Fig 2A). Infection with Δ*hly L. monocytogenes* strikingly showed no increase in PGE_2 over mock-immunized controls (Fig 2A). To ensure that the reduced PGE_2 production was not due to differences in bacterial burdens, mice were infected at a dose of wild-type (10^5 bacteria) and Δ*hly L. monocytogenes* (10^7 bacteria) that led to comparable burdens (Fig 2B). This shows that the absence of PGE_2 in Δ*hly L. monocytogenes*-infected mice is not just due to reduced bacterial burdens. Taken together, these data highlight that cytosolic access is necessary for *in vivo* induction of PGE_2.

$CD11c^+$ and $Lyz2^+$ cells produce PGE_2 during *L. monocytogenes* infection *in vivo*

Our data identified PGE_2 production by macrophages and dendritic cells *ex vivo* (Fig 1D). Furthermore, previous groups have reported that macrophage and dendritic cell subsets are heavily infected early during *in vivo* infection, a timepoint where we have previously detected increases in splenic PGE_2[14,20]. From these data, we next hypothesized that macrophages and/or dendritic cells were responsible for producing PGE_2 *in vivo* that is necessary for optimal T-cell priming. To test this hypothesis, we generated mice deficient in COX-2 selectively in $CD11c^+$ cells or $Lyz2^+$ cells using the cre/lox system. Mice containing *loxP* sites flanking the COX-2-encoding gene ($COX\text{-}2^{fl/fl}$) were crossed with mice expressing the cre recombinase under the CD11c or Lyz2 promoters. $COX\text{-}2^{fl/fl}$ CD11c-cre and $COX\text{-}2^{fl/fl}$ Lyz2-cre mice (subsequently

bioRxiv preprint doi: https://doi.org/10.1101/2021.03.23.436585; this version posted March 23, 2021. The copyright holder for this preprint (which was not certified by peer review) is the author/funder, who has granted bioRxiv a license to display the preprint in perpetuity. It is made available under aCC-BY 4.0 International license.

266 referred to as CD11c-cre and Lyz2-cre) were immunized with 10^7 CFU of a live-attenuated,
267 vaccine strain of *L. monocytogenes* (LADD *L. monocytogenes*) currently used in clinical trials as
268 a cancer therapy platform[24]. The LADD strain is deficient in two major virulence genes, *actA*
269 and *inlB*, that retains immunogenicity while making it safe for clinical use[24]. The vaccine
270 strain was used here to enable analysis of T-cell responses in floxed mice as discussed below and
271 induces similar levels of PGE_2[14]. Immunization of CD11c-cre and Lyz2-cre mice each showed
272 reduced levels of PGE_2 production, leading to only 60% of the PGE_2 induced during
273 immunization of control mice (Fig 3A). However, deletion of COX-2 in either $CD11c^+$ or $Lyz2^+$
274 cells did not abrogate production to the level of mice globally deficient in mPGES-1 (mPGES-$1^{-/-}$)
275 (Fig 3A). This suggests that $CD11c^+$ and $Lyz2^+$ cells each contribute to PGE_2 production and
276 that deletion of COX-2 in either is not sufficient to completely prevent PGE_2 production. We
277 also assessed PGE_2 levels in mice deficient in COX-2 selectively in T-cells and observed no
278 reduction of PGE_2 (S3 Fig). As T-cells are not known to be infected by *L. monocytogenes,* this is
279 consistent with our hypothesis suggesting PGE_2 production specifically from infected cell
280 subsets.
281
282 PGE_2 is critical for generating optimal T-cell responses in response to *L. monocytogenes,* as
283 immunization of mPGES-1-deficient mice or treatment of mice with a COX-2-specific
284 pharmacological inhibitor leads to impaired T-cell responses[14]. We next hypothesized that the
285 decreased PGE_2 production in the CD11c-cre or Lyz2-cre mice would be sufficient to similarly
286 impair T-cell responses. To test this hypothesis, we immunized mice with 10^7 LADD *L.*
287 *monocytogenes* expressing the model antigens B8R and OVA. Seven days after immunization,
288 splenocytes were isolated, stimulated with B8R or OVA, and production of IFN was assessed by

bioRxiv preprint doi: https://doi.org/10.1101/2021.03.23.436585; this version posted March 23, 2021. The copyright holder for this preprint (which was not certified by peer review) is the author/funder, who has granted bioRxiv a license to display the preprint in perpetuity. It is made available under aCC-BY 4.0 International license.

289 flow cytometry. Despite decreased PGE_2 production in these mice, T-cell responses were not
290 affected both in percent IFN^+ as well as number of IFN^+ T-cells per spleen (Fig 3B-C, S4 Fig)
291 Similarly, the number of antigen-specific T-cells measured by B8R tetramer was unchanged in
292 these mice compared to control mice (S4 Fig). This suggests that the PGE_2 remaining in these
293 mice was sufficient to prime productive T-cell responses. Due to its short *in vivo* half-life, PGE_2
294 asserts its effects locally[25]. It is possible that while global splenic PGE_2 levels are decreased,
295 the local concentrations of PGE_2 are sufficient to prime T-cell responses. Taken together, these
296 data suggest that although $Lyz2^+$ and $CD11c^+$ cells contribute to production of PGE_2 during *L.*
297 *monocytogenes* infection, PGE_2 production by these cells is not necessary, as T-cell responses
298 are not impacted by loss of PGE_2 production in either subset.
299
300 **Deletion of COX-2 in both $Lyz2^+$ and $CD11c^+$ cells further reduces splenic PGE_2 levels**
301 Our data showed that single deletions of COX-2 in $CD11c^+$ or $Lyz2^+$ cells reduced PGE_2, but not
302 to baseline values. We next hypothesized that PGE_2 production by either of these subsets
303 individually was sufficient for T-cell priming and that to observe impaired T-cell responses we
304 would have to eliminate PGE_2 production in both $CD11c^+$ and $Lyz2^+$ cells. To do this, we
305 crossed the COX-$2^{fl/fl}$ CD11c-cre and COX-$2^{fl/fl}$ Lyz2-cre mice, leading to mice with a COX-2
306 deletion in both cell subsets (COX-$2^{fl/fl}$ CD11c-cre Lyz2-cre). We assessed the ability of these
307 mice to produce PGE_2 by mass spectrometry and found that PGE_2 was further reduced, with
308 about 40% the amount PGE_2 produced compared to immunized control mice (Fig 4A). This
309 suggests that $CD11c^+$ and $Lyz2^+$ cells produce the majority of PGE_2 during immunization with *L.*
310 *monocytogenes*.
311

bioRxiv preprint doi: https://doi.org/10.1101/2021.03.23.436585; this version posted March 23, 2021. The copyright holder for this preprint (which was not certified by peer review) is the author/funder, who has granted bioRxiv a license to display the preprint in perpetuity. It is made available under aCC-BY 4.0 International license.

Due to further reduced PGE_2 production in our mice deficient in COX-2 in both $CD11c^+$ and $Lyz2^+$ cells, we next assessed T-cell responses in these mice. Mice again were immunized with 10^7 vaccine strain of *L. monocytogenes* expressing the model antigens B8R and OVA and assessed for IFN production seven days later. Despite diminished PGE_2 production, T-cell responses were again not affected, both in percent and number (Fig 4B-C, S5 Fig) Similarly, antigen-specific T-cells measured by B8R tetramer were also unchanged compared to wild-type controls (S5 Fig). This suggest that even the small amount of PGE_2 produced locally is sufficient to drive T-cell responses.

Depletion of phagocytes eliminates PGE_2 production *in vivo*

Our *ex vivo* data highlighted the capability of BMDMs and BMDCs to produce PGE_2 in response to cytosolic *L. monocytogenes*. However, deletion of COX-2 in $Lyz2^+$ and $CD11c^+$ cells did not completely abrogate PGE_2 production *in vivo.* These data led us to hypothesize that other phagocytic cell subsets not effectively targeted by these cre-drivers may be producing the residual PGE_2, such as marginal zone macrophages (MZMs), metallophilic macrophages, or other $CD11b^+$ cells more broadly[26,27]. To test this hypothesis, we utilized short-term clodronate liposomes to rapidly deplete phagocyte populations in the spleen. Mice were depleted with clodronate liposomes 24 hours prior to immunization with *L. monocytogenes*[28]. Twelve hours post immunization, spleens were harvested and assessed for PGE_2 by mass spectrometry. Additionally, splenocytes were assessed for $CD11b^+$ and $CD11c^+$ populations by flow cytometry to confirm clodronate efficacy. Clodronate treatment led to significantly fewer $CD11b^+$ cells and a trend for decreased $CD11c^+$ cells (S6 Fig). Treatment of mice with clodronate prior to infection with *L. monocytogenes* completely eliminated PGE_2 production compared to infected control

bioRxiv preprint doi: https://doi.org/10.1101/2021.03.23.436585; this version posted March 23, 2021. The copyright holder for this preprint (which was not certified by peer review) is the author/funder, who has granted bioRxiv a license to display the preprint in perpetuity. It is made available under aCC-BY 4.0 International license.

mice (Fig 5A). Importantly, bacterial burdens were equivalent between clodronate and mock-treated mice (Fig 5B). Pretreatment with a control empty liposome, encapsome, actually increased PGE_2 production compared to infected control mice, potentially due to increased bacterial burdens (Fig 5A-B). Taken together, these data demonstrate that phagocytic cell populations are critical for PGE_2 production *in vivo* following *L. monocytogenes* immunization.

Loss of antigen presenting cells through clodronate treatment leads to impaired $CD8^+$ T-cell activation, making analysis of T-cell responses in this model not informative[29,30]. Given this, we alternatively assessed the possibility that other phagocytic cells targeted by clodronate, but not the Lyz2-cre, could contribute to PGE_2 production. Complete elimination of PGE_2 production with clodronate treatment suggested that the residual PGE_2 in the CD11c-cre Lyz2-cre mice was due to a phagocytic cell that was not effectively targeted in these mice. Previous data showed that though the Lyz2-cre used in this study is highly efficient at deletion of *loxP* flanked genes in some macrophage subsets, it is only minimally successful at deleting genes of interest in other subsets, such as MZMs[26]. MZMs, characterized by expression of MARCO, are heavily infected early in *L. monocytogenes* infection[20]. We hypothesized that the residual PGE_2 we detected in our double CD11c-cre and Lyz2-cre mice may be due to inefficient deletion in macrophage subsets such as these. To assess the role of MZMs in PGE_2 production, we assessed expression of COX-2 by immunohistochemistry. Mice were immunized with 10^7 vaccine strain of *L. monocytogenes* and spleens were harvested three and ten hours later. Spleen cryosections were then stained for *L. monocytogenes*, COX-2, and MARCO. Uninfected mice had COX-2 staining in the periarteriolar lymphoid sheath (PALS) with little expression in the marginal zone (MZ) (Fig 5C,-D). As early as three hours post-immunization COX-2 staining was observed in

bioRxiv preprint doi: https://doi.org/10.1101/2021.03.23.436585; this version posted March 23, 2021. The copyright holder for this preprint (which was not certified by peer review) is the author/funder, who has granted bioRxiv a license to display the preprint in perpetuity. It is made available under aCC-BY 4.0 International license.

the MZ, with approximately 50% of COX-2 colocalizing with $MARCO^+$ cells (Fig 5C-D). Expression of COX-2 in the MZ was maintained at 10hpi, again showing approximately 50% colocalization with MARCO (Fig 5C-D). Furthermore, *L. monocytogenes* colocalized with COX-2 and MARCO expressing cells, suggesting that infected MZMs may be producing PGE_2 (Fig 5D). Expression of COX-2 suggests that MZMs, or other non-CD11c/Lyz2 expressing phagocytes within the marginal zone, could be capable of producing PGE_2 *in vivo* and may be contributing to the PGE_2 remaining in the CD11c-cre Lyz2-cre mice. Taken together, our data suggest that multiple myeloid derived subsets can contribute to PGE_2 production, including $Lyz2^+$ cells, $CD11c^+$ cells, and possibly MZMs. Complete reductions in PGE_2 by depletion of phagocytic cells such as these with clodronate treatment is consistent with our data showing that PGE_2 is produced from cells infected with cytosolic *L. monocytogenes.*

bioRxiv preprint doi: https://doi.org/10.1101/2021.03.23.436585; this version posted March 23, 2021. The copyright holder for this preprint (which was not certified by peer review) is the author/funder, who has granted bioRxiv a license to display the preprint in perpetuity. It is made available under aCC-BY 4.0 International license.

Discussion

Cytosolic access is required to effectively generate cell-mediated immunity to *L. monocytogenes*[8–10]. Decades of work has focused on understanding the cytosol-dependent processes necessary for T-cell priming, a topic that has gained interest recently due to use of *L. monocytogenes* as a cancer immunotherapy platform. Our data suggest that one reason cytosolic access is important is to facilitate phagocyte production of PGE_2, an eicosanoid required to generate optimal $CD8^+$ T-cell responses[14]. We showed that PGE_2 is produced by BMDMs and BMDCs *ex vivo*. Importantly, this pathway requires cytosolic access, as vacuole-constrained *L. monocytogenes* induce lower production of PGE_2. Furthermore, infection of mice with a vacuole-constrained *L. monocytogenes* strain led to no increase of PGE_2 over mock immunized controls. Lastly, we showed that $Lyz2^+$ and $CD11c^+$ cells contribute to PGE_2 production *in vivo* as deletion of COX-2 in these subsets led to decreased PGE_2 levels, however other clodronate sensitive phagocyte populations also contribute to PGE_2 production following *L. monocytogenes* immunization. We demonstrate the first-known innate pathway critical for $CD8^+$ T-cell responses that requires cytosolic access by *L. monocytogenes*. This work leads to many new questions including how cytosolic *L. monocytogenes* activates this pathway, how immune cells discriminate which eicosanoid to produce in response to infection, how even small concentrations of PGE_2 still lead to productive PGE_2 responses, and how PGE_2 facilitates optimal T-cell priming.

One intriguing hypothesis is that PGE_2 synthesis during *L. monocytogenes* infection is driven by an innate cytosolic sensor. *L. monocytogenes* elicits a number of innate pathways that could contribute to differential activation of the PGE_2-synthesis pathway. One possibility is that induction of type I IFN influences PGE_2 production. Type I IFN can be induced cytosolically by

bioRxiv preprint doi: https://doi.org/10.1101/2021.03.23.436585; this version posted March 23, 2021. The copyright holder for this preprint (which was not certified by peer review) is the author/funder, who has granted bioRxiv a license to display the preprint in perpetuity. It is made available under aCC-BY 4.0 International license.

392 *L. monocytogenes* through recognition of cyclic diadenosine monophosphate (c-di-AMP). Upon
393 entry into the cytosol, *L. monocytogenes* secretes c-di-AMP through multidrug resistance
394 transporters[31,32] where it is recognized by either the reductase controlling NF-κB
395 (RECON)[33] or stimulator of IFN genes (STING)[34,35]. STING activation leads to type I
396 interferon induction[34,35], and was originally hypothesized to be critical for T-cell responses.
397 Paradoxically, however, type I IFN inhibits cell-mediated immunity to *L. monocytogenes*[12].
398 Interestingly, there has been well documented crosstalk between the PGE_2 and type I IFN
399 pathways during infections with other pathogens such as influenza and *M. tuberculosis*[36,37].
400 In the context of influenza, Coulombe et al. showed that infection led to upregulation of PGE_2
401 and a subsequent decrease in type I IFN[36]. In contrast to *L. monocytogenes,* type I IFN is
402 important in generating cell-mediated immune responses to influenza. Accordingly, diminished
403 type I IFN due to increased PGE_2 reduces both acute and protective immunity during influenza
404 infection. On the other hand, Mayer-Barber et al. recently showed that inhibition of type I IFN
405 during *M. tuberculosis* infection led to an increased level of PGE_2 in an IL-1-dependent
406 manner[37]. This correlated with better bacterial control. Due to crosstalk between these two
407 pathways, it seems possible that recognition of c-di-AMP and subsequently upregulation of type
408 I IFN may also be playing a role in PGE_2 production during *L. monocytogenes* immunization.
409 Analysis of PGE_2 levels in mice deficient in STING or the type I IFN receptor (IFNAR) could
410 advance understanding of the link between these two pathways. Alternatively, should type I IFN
411 influence PGE_2 production, use of *L. monocytogenes* strains that have reduced secretion of c-di-
412 AMP and subsequently less type I IFN could be an avenue of further research for
413 immunotherapeutic platforms.

bioRxiv preprint doi: https://doi.org/10.1101/2021.03.23.436585; this version posted March 23, 2021. The copyright holder for this preprint (which was not certified by peer review) is the author/funder, who has granted bioRxiv a license to display the preprint in perpetuity. It is made available under aCC-BY 4.0 International license.

Another cytosolic pathway that may influence PGE_2 levels during *L. monocytogenes* infection is the inflammasome. Inflammasomes are multiprotein complexes that recognize a wide range of pathogen associated molecular patterns[38–40]. Wild-type *L. monocytogenes* infection leads to a small amount of inflammasome activation, largely through the absent in melanoma 2 (AIM2) inflammasome[41]. The AIM2 inflammasome recognizes cytosolic DNA that is released during bacteriolysis within the cytosol[41–43]. Originally, inflammasomes such as AIM2 were known to have two major downstream effects, the release of proinflammatory cytokines IL1β/IL-18 and the induction of a lytic form of cell death, pyroptosis, characterized by formation of membrane pores by the protein Gasdermin D[44–46]. Seminal work by von Moltke et al. introduced a new downstream effect, the activation of an eicosanoid storm, including PGE_2[23]. This work, as well as supporting recent work, showed elevated levels of PGE_2 after inflammasome activation[23,47]. One possible hypothesis stemming from this work is that induction of membrane pores during pyroptosis leads to calcium influx, activating cPLA2 and releasing arachidonic acid from the membrane. This model would suggest that use of mice deficient in caspase-1 or Gasdermin D would lead to lower levels of PGE_2 production. Alternatively, infection of *L. monocytogenes* strains that differentially activate inflammasomes would lead to different PGE_2 production. The role of inflammasomes as well as type I IFN are intriguing avenues to understand signaling pathways driving PGE_2 production during *L. monocytogenes* infection.

It is also possible that production of PGE_2 by *L. monocytogenes* is independent of known cytosolic pathways. Identification of other unknown censors could be accomplished by assessing PGE_2 levels in response to different *L. monocytogenes* mutants. Mutant strains of *L. monocytogenes* that differentially induce PGE_2 could provide insight as to the cytosolic censors

bioRxiv preprint doi: https://doi.org/10.1101/2021.03.23.436585; this version posted March 23, 2021. The copyright holder for this preprint (which was not certified by peer review) is the author/funder, who has granted bioRxiv a license to display the preprint in perpetuity. It is made available under aCC-BY 4.0 International license.

involved. One additional hypothesis is that PGE_2-production is independent of a cytosolic sensor completely and instead is driven by LLO-mediated pore formation. Though LLO is tightly regulated transcriptionally, translationally, and posttranslationally to be most active in the vacuole, a small amount of LLO may remain active in the cytosol of cells[48–50]. Perhaps, this small amount of LLO induces pore formation in the cell membrane and allows calcium influx, subsequently activating cPLA2. Use of strains that further restrict LLO production in the cytosol, such as new strains that excise *hly* once *L. monocytogenes* has entered the cytosol[51], could help assess the role of LLO-mediated pores on PGE_2 production.

In addition, our data show an interesting phenotype where BMDCs and PAM-primed BMDMs selectively produce PGE_2 in response to *L. monocytogenes* infection rather than a global increase in eicosanoid production. Analysis of eicosanoid milieu in cell supernatant show an increase in PGE_2 production during wild-type *L. monocytogenes* infection, but little to no changes in other eicosanoids such as PGD_2, TXB_2, or LTB_4. This raises the question of how a cell discriminates which eicosanoid is produced in response to different stimuli. The eicosanoid produced in different conditions is dependent on terminal synthases[19]. Therefore, the expression and activity of these synthases determine the resulting eicosanoid milieu. Multiple factors impact expression of different synthases including cytokines, hormones, and microbial products[52]. For example, expression of mPGES-1 can be induced by LPS and prostaglandin D_2 synthases, though less well understood, can be upregulated by glucocorticoids[53–55]. Use of *L. monocytogenes* strains that differentially activate cytokines or are deficient in different microbial PAMPs could be informative as to which signal specifically leads to enhanced levels of mPGES-1 transcript. In addition, activity of each synthase also may dictate which eicosanoids are produced[52]. Terminal synthase activity can be modulated by posttranslational modification

bioRxiv preprint doi: https://doi.org/10.1101/2021.03.23.436585; this version posted March 23, 2021. The copyright holder for this preprint (which was not certified by peer review) is the author/funder, who has granted bioRxiv a license to display the preprint in perpetuity. It is made available under aCC-BY 4.0 International license.

(such as phosphorylation) as well as presence of cofactors (such as ATP and glutathione)[52]. Depletion of essential cofactors during metabolic or oxidative stress could influence the induced inflammatory milieu[52]. The post transcriptional regulation highlights the necessity of assessing endpoint eicosanoid production rather than simply transcript or protein levels, as these other factors influencing activity can alter which eicosanoids ultimately are produced. This is particularly true in our data, as despite seeing upregulation of mPGES-1 transcript during infection of unprimed BMDMs and BMDCs, we failed to see PGE_2 production. This suggests that perhaps some additional modification is necessary to induce mPGES-1 activity during *L. monocytogenes* infection.

Another pressing question generated from this work is how productive T-cell responses were induced in mice deficient in COX-2 in both $CD11c^+$ and $Lyz2^+$ cells despite reduced PGE_2 levels. Here, we show that these mice produce substantially reduced PGE_2, yet still induce wild-type $CD8^+$ T-cell responses. One hypothesis that we explored in this work is that other cell subsets not efficiently targeted by our cre/lox model were still producing PGE_2. Certain cell subsets such as MZMs do not have effective gene deletion using the $Lyz2^+$ promoter to drive cre recombinase expression[26]. For this reason, we hypothesized that subsets such as these may still be producing sufficient levels of PGE_2 to drive T-cell responses. One way to assess the role of $MARCO^+$ MZMs is use of a new cre recombinase-driving promoter, SIGN-R1, developed by Pirgova et al[27]. SIGN-R1 is a lectin binding receptor expressed on MZMs and drives more efficient deletion of genes by the cre/lox system[27]. Generation of triple COX-2 knockout mice that express the SIGN-R1-cre in combination with our reported Lyz2-cre CD11c-cre model could be informative about the role of MZMs in production of PGE_2. Though we show that

bioRxiv preprint doi: https://doi.org/10.1101/2021.03.23.436585; this version posted March 23, 2021. The copyright holder for this preprint (which was not certified by peer review) is the author/funder, who has granted bioRxiv a license to display the preprint in perpetuity. It is made available under aCC-BY 4.0 International license.

482 Lyz2$^+$ and CD11c$^+$ cells contribute to PGE_2, analysis of MZMs and other myeloid cells will
483 further understanding of PGE_2 production.

484 The lack of diminished cell-mediated immunity could also be due to local acting effects
485 of PGE_2. It is possible that even if PGE_2 levels are below detection at a whole spleen level,
486 certain cells are able to produce PGE_2 locally in sufficient concentration to drive T-cell
487 responses. More sensitive measures of PGE_2, such as quantitative mass spectrometry imaging
488 recently developed, would be required to analyze local responses such as these[56]. These novel
489 techniques enable analysis of location of PGE_2 and other eicosanoids within a spleen and could
490 detect lower concentrations[56]. Similarly, the sensitivity of the receptor PGE_2 is acting upon
491 during *L. monocytogenes* infection could influence how much PGE_2 is necessary for inducing a
492 response. PGE_2 binds primarily to four receptors, EP1-4[57]. EP3 and EP4 are higher affinity
493 receptors (kD ~1nM compared to 10-15nM for EP1/2)[57,58]. Should the higher affinity
494 receptors be identified as the important receptors for influencing immunity during *L.*
495 *monocytogenes* infection, even lower concentrations of PGE_2 still induced in our Lyz2-cre
496 CD11c-cre model may be sufficient for cell-mediated responses. Further analysis as to relevant
497 receptors and which cells they are expressed on could help elucidate these details.

498 Lastly, how PGE_2 facilitates T-cell responses in the context of *L. monocytogenes*
499 immunization remains unknown. In innate immune cells, PGE_2 influences expression of co-
500 stimulatory and activation markers. PGE_2 signaling in dendritic cells upregulates the co-
501 stimulatory molecules OX40L and 4-1BBL[59], thereby promoting T-cell proliferation.
502 Similarly, PGE_2 signaling in macrophages leads to polarization towards a more inflammatory
503 M1 phenotype[60] and aids in activation[61]. Furthermore, PGE_2 promotes migration of innate
504 cell subsets, leading to enhanced migration towards CCL21[62,63] and MCP-1[64,65]. These

bioRxiv preprint doi: https://doi.org/10.1101/2021.03.23.436585; this version posted March 23, 2021. The copyright holder for this preprint (which was not certified by peer review) is the author/funder, who has granted bioRxiv a license to display the preprint in perpetuity. It is made available under aCC-BY 4.0 International license.

505 proinflammatory functions suggest that PGE_2 may be acting to enhance immunity through its
506 local effects on innate immune cells. PGE_2 may also be influencing immunity more directly on
507 T-cell subsets, such as through polarization of T-cells towards a Th1 phenotype[66].
508 Additionally, PGE_2 leads to higher expression of OX-40L, OX-40, and CD70 directly on T-cells,
509 promoting T-cell interactions and sustaining immune responses[59]. In order to more fully
510 understand how PGE_2 facilitates T-cell responses to *L. monocytogenes*, a comprehensive analysis
511 of these effects on both T-cells and innate immune cells is required.
512 We and others have shown that innate immune responses substantially influence cell-
513 mediated immune responses, particularly the inflammatory milieu induced during infection.
514 Here, we present evidence that one pathway critical for immunity, induction of PGE_2, is
515 dependent on access to the cytosol. Furthermore, we show that PGE_2 is produced by
516 macrophages and dendritic cells. These data provide new insight as to how $CD8^+$ T-cells are
517 primed as well as suggest analysis and modulation of eicosanoid levels, particularly PGE_2 levels,
518 may be informative to improve the use of *L. monocytogenes*-based immunotherapeutic
519 platforms.
520

bioRxiv preprint doi: https://doi.org/10.1101/2021.03.23.436585; this version posted March 23, 2021. The copyright holder for this preprint (which was not certified by peer review) is the author/funder, who has granted bioRxiv a license to display the preprint in perpetuity. It is made available under aCC-BY 4.0 International license.

Materials and Methods

Ethics statement: This work was carried out in strict accordance with the recommendations in the Guide for the Care and Use of Laboratory Animals of the National Institutes of Health. All protocols were reviewed and approved by the University of Wisconsin-Madison Institutional Animal Care and Use Committee.

Bacterial strains: The *Listeria monocytogenes* strains used in this study were all in the 10403s background. The attenuated (LADD) strain used in the analysis of T-cell responses was in the Δ*actA*Δ*inlB* background as previously described and engineered to express full length OVA and the $B8R_{20-27}$ epitope[24]. OVA and $B8R_{20-27}$ were constructed as a fusion protein under the control of the *actA* promoter with the secretion signal of the amino terminal 300bp of the ActA gene[13]. This fusion protein was integrated into the site-specific pPL2e vector as previously described[13].

Mouse strains: Six- to eight-week-old C57BL/6 male and female mice were obtained from the NCI and Charles River NCI facility. *Ptgs2*$^{-/-}$ (COX-2$^{-/-}$) mice were obtained from Jackson Laboratory and maintained as heterozygote breeding pairs. *Ptges*$^{-/-}$ (mPGES1$^{-/-}$) mice lacking microsomal PGE synthase have been previously described[67–69]. In order to generate cell-type specific COX-2 knockout mice, COX-2$^{fl/fl}$ mice (stock number 030785) were obtained from Jackson Laboratory and crossed with Lyz2-cre (stock number 004781), CD11c-cre (stock number 008068), or CD4-cre expressing mice (stock number 022071), all also obtained from Jackson Laboratory. Double Lyz2-cre and CD11c-cre expressing mice were generated by

bioRxiv preprint doi: https://doi.org/10.1101/2021.03.23.436585; this version posted March 23, 2021. The copyright holder for this preprint (which was not certified by peer review) is the author/funder, who has granted bioRxiv a license to display the preprint in perpetuity. It is made available under aCC-BY 4.0 International license.

crossing COX-$2^{fl/fl}$ Lyz2-cre mice with COX-$2^{fl/fl}$ CD11c-cre mice. Genotypes were confirmed by PCR using the primer pairs in Table 1.

Table 1. Genotyping primers

Mouse genotype	Forward (5'-3')	Reverse (5'-3')
COX-$2^{fl/fl}$	AAT TAC TGC TGA AGC CCA CC	CTT CCC AGC TTT TGT AAC CAT
CD4-cre	GAACC TGATG GACAT GTTCA GG TTACG TCCAT CGTGG ACAGC (internal control)	AGTGC GTTCG AACGC TAGAG CCTGT TGGGC TGGGT GTTAG CCTTA (internal control)
CD11c-cre	ACT TGG CAG CTG TCT CCA AG CAA ATG TTG CTT GTC TGG TG (internal control)	GCG AAC ATC TTC AGG TTC TG GTC AGT CGA GTG CAC AGT TT (internal control)
Lyz2-cre	CCC AGA AAT GCC AGA TTA CG	CTT GGG CTG CCA GAA TTT CTC

BMDM and BMDC generation and infection: Bone marrow-derived macrophages and dendritic cells were made using six- to eight-week-old *Ptgs2*$^{-/-}$ (COX-$2^{-/-}$) or C57BL/6 mice as previously described[13,70]. Briefly, bone marrow was harvested and macrophages were cultured in the presence of M-CSF from transfected 3T3 cell supernatant for six days with a supplement of M-CSF at day three and frozen down for storage. Dendritic cells were cultured in the presence of 20ng/ml recombinant GM-CSF (BD Biosciences, San Jose, CA) for 7 days with a supplement of 20ng/mL GM-CSF every third day. For infection, BMDMs or BMDCs were plated at $1x10^6$ cells/well in a 12 well dish overnight +/- 100ng/mL PAM3CSK4. The following morning, cells were infected with indicated strains of *L. monocytogenes* or PBS control at an MOI of 10. Thirty minutes later, supernatant was removed and replaced with medium containing 50μg/mL gentamycin to remove extracellular bacteria. Six hours post infection, cells were

bioRxiv preprint doi: https://doi.org/10.1101/2021.03.23.436585; this version posted March 23, 2021. The copyright holder for this preprint (which was not certified by peer review) is the author/funder, who has granted bioRxiv a license to display the preprint in perpetuity. It is made available under aCC-BY 4.0 International license.

558 harvested for western blot or qRT PCR and supernatant was harvested for eicosanoid analysis as
559 described below.
560
561 **qRT PCR:** RNA was isolated from BMDMs or BMDCs using the RNAqueous-Micro Total
562 RNA Isolation Kit (Invitrogen), and DNAse treated with Turbo DNAse (Invitrogen) according to
563 manufacturer's instructions. 500ng total RNA was reverse transcribed in 10µL reactions using
564 the iScript cDNA Synthesis Kit (BioRad) according to manufacturer's instructions and cDNA
565 was diluted 10-fold using molecular grade water (Invitrogen). 2.5µL diluted cDNA was used as
566 template in a 10µL qRT-PCR reaction performed in duplicate using gene-specific primers and
567 Kapa SYBR Green Universal qPCR mix (KAPA Biosystems) according to manufacturer's
568 instructions using a BioRad CFX Connect Real-Time PCR System. The sequences of gene-
569 specific primers are shown in Table 2. Data was analyzed using Excel and all RNA abundances
570 were calculated by using a standard curve of synthesized template (Integrated DNA
571 Technologies, G-Blocks) and are normalized to *ActB* (β-actin).

572 **Table 2. qRT PCR primers**

Gene	Forward (5'-3')	Reverse (5'-3')
ActB	AAT TAC TGC TGA AGC CCA CC	CTT CCC AGC TTT TGT AAC CAT
Ptgs2	GAACC TGATG GACAT GTTCA GG TTACG TCCAT CGTGG ACAGC (internal control)	AGTGC GTTCG AACGC TAGAG CCTGT TGGGC TGGGT GTTAG CCTTA (internal control)
Ptges	ACT TGG CAG CTG TCT CCA AG CAA ATG TTG CTT GTC TGG TG (internal control)	GCG AAC ATC TTC AGG TTC TG GTC AGT CGA GTG CAC AGT TT (internal control)
Pla2g4a	CCC AGA AAT GCC AGA TTA CG	CTT GGG CTG CCA GAA TTT CTC
Ifnb1	GCACTGGGTGGAATGAGACTATTG	TTCTGAGGCATCAACTGACAGGTC
Il1b	GACCTGTTCTTTGAAGTTGACGG	TGTCGTTGCTTGGTTCTCCTTG

bioRxiv preprint doi: https://doi.org/10.1101/2021.03.23.436585; this version posted March 23, 2021. The copyright holder for this preprint (which was not certified by peer review) is the author/funder, who has granted bioRxiv a license to display the preprint in perpetuity. It is made available under aCC-BY 4.0 International license.

Western blots: BMDMs or BMDCs were harvested and protein was extracted using the Pierce SDS-PAGE Sample Prep Kit (Thermo) according to the manufacturer's instructions. Total protein content was measured by the Pierce BCA Protein Assay Kit (Thermo) and equivalent protein levels were loaded into an polyacrylamide gel (BioRad). Samples were transferred onto a nitrocellulose membrane using a semi-dry transfer apparatus before blocking with a 5% skim milk solution for thirty minutes at room temperature. After washing 3x with PBS-T, the membrane was incubated overnight at 4°C with the primary antibodies anti-COX-2 (1:200, Cayman Chemical) and anti-β-actin loading control (1:1000, ThermoFisher) in a 5% bovine serum albumin solution. The following day samples were washed with PBS-T before being incubated with secondary antibodies (anti-rabbit 800 at 1:10,000, anti-mouse 680 at 1:5,000). Samples were imaged on a LiCor imager and analyzed via ImageStudio. Sample signal was normalized to β-actin and relative abundance was compared to wild-type *L. monocytogenes.*

***In vivo* immunizations and pharmacological treatments:** *L. monocytogenes* of the wild-type, attenuated (LADD), or *Δhly* background were grown overnight in brain heart infusion media at 30C. The bacteria were back diluted 1:5 and allowed to grow to log phase (OD0.4-0.6, ~1-1.5 hours) at 37C, with aeration, prior to infection. Bacteria were diluted in PBS and mice were infected with 200µL at the indicated doses intravenously. For bacterial burden analysis, mice were sacrificed at 12hpi and livers were homogenized in 0.1% Nonidet P-40 in PBS and plated on Luria-Bertani plates. For splenic macrophage depletion, 200µL clodronate, PBS control, or endosome lipid control (Encapsula Nano Sciences) were given intravenously 24 hours prior to bacterial infection according to the manufacturer's instructions. Depletion efficacy was

bioRxiv preprint doi: https://doi.org/10.1101/2021.03.23.436585; this version posted March 23, 2021. The copyright holder for this preprint (which was not certified by peer review) is the author/funder, who has granted bioRxiv a license to display the preprint in perpetuity. It is made available under aCC-BY 4.0 International license.

596 confirmed by assessing abundance of splenic $CD11b^+$ cells (clone M1/70) and $CD11c^+$ cells
597 (clone N418) by flow cytometry. Celecoxib (Cayman Chemical) was milled into standard mouse
598 chow (Envigo) at 100mg/kg and fed ad lib for 48 hours before and after immunization[14,71].
599
600 **Eicosanoid measurement:** For *in vivo* eicosanoid extractions, spleens from mice were harvested
601 at twelve hours post immunization and flash frozen in tubes containing 50ng deuterated PGE_2
602 standard (Cayman Chemical) in 5μL methanol and stored overnight at -80C. For *ex vivo*
603 extractions, 1mL of supernatant was flash frozen in tubes similarly containing 50ng deuterated
604 PGE_2 standard in 5μL methanol. The following day, two mL of ice cold methanol were added to
605 the tissue culture supernatant or spleens. Spleens were homogenized in glass homogenizers.
606 Samples then were incubated at 4C for 30 minutes. Next, cellular debris was removed by
607 centrifugation and samples were concentrated to 1mL volume before being acidified with pH 3.5
608 water and loaded onto conditioned solid phase C18 cartridges. Samples were washed with
609 hexanes before eluting using methyl formate followed by methanol. Samples were concentrated
610 using a steady stream of nitrogen gas and suspended into 55:45:0.1 MeOH:H_2O:acetic acid and
611 analyzed on an HPLC coupled to a mass spectrometer (Q Exactive; Thermo Scientific) using a
612 C18 Acquity BEH column (100mm x 2.1 mm x 1.7μm) operated in negative ionization mode.
613 Samples were eluted with a mobile phase 55:45:0.1 MeOH:H_2O:acetic acid shifted to 98:2:0.1
614 over 20 minutes. Mass-to-charge ratios included were between 100 and 800 and compared to
615 standards (Cayman Chemical) by analysis via MAVEN.
616
617 **T-cell analysis:** Mice were sacrificed seven days after immunization and splenocytes were
618 isolated as previously described[4]. In brief, red blood cells were lysed using ACK buffer and

bioRxiv preprint doi: https://doi.org/10.1101/2021.03.23.436585; this version posted March 23, 2021. The copyright holder for this preprint (which was not certified by peer review) is the author/funder, who has granted bioRxiv a license to display the preprint in perpetuity. It is made available under aCC-BY 4.0 International license.

then splenocytes were counted using a Z1 Coulter counter. For tetramer analysis, splenocytes were immediately blocked for Fc (Tonbo Bioscience) and stained for B8R tetramer (AF488, 1:300, NIH Tetramer Facility, Atlanta, GA) followed by staining with anti-CD3 (PeCy7, 1:100, clone 145-2C11) and anti-CD8α (eFlour450, 1:200, clone 145-2C11). Cells were then stored overnight at 4C in a 1:1 of IC Fixation Buffer (ThermoFisher Scientific) and FACS buffer. For analysis of cytokine production, $1.7x10^6$ cells were plated in a 96 well dish and incubated for five hours in the presence of $B8R_{20-27}$ (TSYKFESV) or $OVA_{257-264}$ (SIINFEKL) peptides and brefeldin A (eBioscience). Splenocytes were then subjected to FC block (Tonbo Bioscience) and stained with anti-CD3 (FITC, 1:200, clone 145-2C11) and anti-CD8α (eFlour450, 1:200, clone 53-6.7) before treatment with fixing and permeabilization buffers (eBioscience). Cells were then further stained with anti-IFNγ (APC, 1:300, clone XMG1.2). Samples were acquired using the LSRII flow cytometer (BD Biosciences, San Jose, CA) and analyzed with FlowJo software (Tree Star, Ashland, OR).

Cryosection preparation and immunofluorescence microscopy of infected spleens: C57BL/6 mice were infected intravenously by tail vein injection of 10^7 LADD *L. monocytogenes* in 150 µl of PBS. Mice were sacrificed at 3 or 10 hpi and spleens harvested and snap frozen in OCT for immunofluorescence microscopy as described previously[20]. Uninfected mice were used as negative controls. Briefly, 5µm spleen cryosections were cut using a Leica CM1850 cryostat, mounted on Superfrost Plus microscope slides (Thermo Fisher) and stored at -80°C until use. Slides were fixed in 10% buffered formalin phosphate at RT for 5 minutes and sections, washed in TBS and blocked with StartingBlock T20 Blocking buffer containing Fc blocker (Thermo Scientific, 37543). Sections were incubated with unconjugated *L. monocytogenes*

bioRxiv preprint doi: https://doi.org/10.1101/2021.03.23.436585; this version posted March 23, 2021. The copyright holder for this preprint (which was not certified by peer review) is the author/funder, who has granted bioRxiv a license to display the preprint in perpetuity. It is made available under aCC-BY 4.0 International license.

642 monoclonal Ab (Invitrogen, MA1-20271), anti-MARCO polyclonal Goat IgG-Biotin (R&D
643 Systems, BAF2956), and FITC-conjugated COX2 polyclonal antibody (Cayman Chemical,
644 10010096) at 1/100-200 dilution at RT for 1-2h in dark humidified incubation chamber or
645 isotype control antibodies including Rabbit IgG-FITC (Invitrogen, 11-4614-80), Armenian
646 Hamter IgG-PE (Invitrogen, 13-4888-81) and Mouse IgG2a kappa (Invitrogen, 14-4724-81).
647 Biotinylated and unconjugated primary antibodies were detected by incubating with
648 Streptavidin-PE (Pharmingen, 534061) and Rat anti-mouse IgG2a antibody (Invitrogen, 17-
649 4210-80) respectively. Slides were preserved using ProLong Diamond Antifade mounting media
650 (Invitrogen, P36965) and clear nail polish to seal the edges. Slides were analyzed using an
651 Olympus IX51 fluorescence microscope equipped with LCPlanFL 20x/0.4 NA and UPlanFL
652 40x/1.3 oil objectives, an X-Cite 120 excitation unit (Exfo), FITC/PE/APC optimized filter sets
653 (Semrock), an Orca Flash 2.8 monochrome camera (Hamamatsu) and SlideBook software
654 (Intelligent Imaging Innovations) for hardware control and image acquisition. Images were
655 captured with both 20x an 40x objective with exposure times ranging from 200-400ms. Pseudo-
656 colored 3-channel RGB mages were imported into Imaris 9.6 (Bitplane) for smoothing, contrast
657 enhancement (linear contrast stretch), annotation and colocalization analysis.
658
659 **Statistical analysis:** Statistical analysis was performed by GraphPad Prism Software (La Jolla,
660 CA) and analyzed via Mann Whitney *U* test or one-way ANOVA with Bonferroni's correction as
661 indicated.
662

bioRxiv preprint doi: https://doi.org/10.1101/2021.03.23.436585; this version posted March 23, 2021. The copyright holder for this preprint (which was not certified by peer review) is the author/funder, who has granted bioRxiv a license to display the preprint in perpetuity. It is made available under aCC-BY 4.0 International license.

Acknowledgments

We would like to thank the NIH Tetramer Core Facility for provision of MHC-I B8R tetramers.

bioRxiv preprint doi: https://doi.org/10.1101/2021.03.23.436585; this version posted March 23, 2021. The copyright holder for this preprint (which was not certified by peer review) is the author/funder, who has granted bioRxiv a license to display the preprint in perpetuity. It is made available under aCC-BY 4.0 International license.

References

1. Rolhion N, Cossart P. How the study of Listeria monocytogenes has led to new concepts in biology [Internet]. Vol. 12, Future Microbiology. Future Medicine Ltd.; 2017. p. 621–38.
2. Le DT, Dubenksy TW, Brockstedt DG. Clinical development of Listeria monocytogenes-based immunotherapies. Semin Oncol. 2012 Jun;39(3):311–22.
3. Corbin GA, Harty JT. Duration of Infection and Antigen Display Have Minimal Influence on the Kinetics of the CD4 + T Cell Response to Listeria monocytogenes Infection . J Immunol. 2004 Nov 1;173(9):5679–87.
4. Theisen E, Sauer JD. Listeria monocytogenes-Induced Cell Death Inhibits the Generation of Cell-Mediated Immunity. Freitag NE, editor. Infect Immun. 2017 Jan;85(1):e00733-16.
5. Richer MJ, Nolz JC, Harty JT. Pathogen-specific inflammatory milieux tune the antigen sensitivity of CD8(+) T cells by enhancing T cell receptor signaling. Immunity. 2013 Jan;38(1):140–52.
6. Portnoy DA, Jacks PS, Hinrichs DJ. Role of hemolysin for the intracellular growth of Listeria monocytogenes. J Exp Med. 1988 Apr 1;167(4):1459–71.
7. Hamon MA, Ribet D, Stavru F, Cossart P. Listeriolysin O: the Swiss army knife of Listeria. Trends Microbiol. 2012 Aug;20(8):360–8.
8. Michael Brunt L, Portnoy DA, Unanue4 ER. Presentation of Listeria Monocytogenes To CD8+ T Cells Requires Secretion of Hemolysin and Intracellular Bacterial Growth'. J Immunol. 2016;145(11).
9. Bahjat KS, Meyer-Morse N, Lemmens EE, Shugart JA, Dubensky TW, Brockstedt DG, et al. Suppression of cell-mediated immunity following recognition of phagosome-confined

bioRxiv preprint doi: https://doi.org/10.1101/2021.03.23.436585; this version posted March 23, 2021. The copyright holder for this preprint (which was not certified by peer review) is the author/funder, who has granted bioRxiv a license to display the preprint in perpetuity. It is made available under aCC-BY 4.0 International license.

bacteria. PLoS Pathog. 2009 Sep;5(9):e1000568.

10. Berche P, Gaillard JL, Sansonetti PJ. Intracellular growth of Listeria monocytogenes as a prerequisite for in vivo induction of T cell-mediated immunity. J Immunol. 1987 Apr 1;138(7):2266–71.

11. Auerbuch V, Brockstedt DG, Meyer-Morse N, O'Riordan M, Portnoy DA. Mice Lacking the Type I Interferon Receptor are Resistant to Listeria monocytogenes. J Exp Med. 2004 Aug 16;200(4):527–33.

12. Archer KA, Durack J, Portnoy DA. STING-dependent type I IFN production inhibits cell-mediated immunity to Listeria monocytogenes. PLoS Pathog. 2014 Jan;10(1):e1003861.

13. Sauer J, Pereyre S, Archer KA, Burke TP, Hanson B, Lauer P, et al. Listeria monocytogenes engineered to activate the Nlrc4 inflammasome are severely attenuated and are poor inducers of protective immunity. Proc Natl Acad Sci U S A. 2011 Jul 26;108(30):12419–24.

14. Theisen E, McDougal C, Nakanishi M, Stevenson DM, Amador-Noguez D, Rosenberg DW, et al. Cyclooxygenase-1 and -2 Play Contrasting Roles in Listeria monocytogenes Stimulated Immunity. J Immunol. 2018;

15. Harizi H, Corcuff J-B, Gualde N. Arachidonic-acid-derived eicosanoids: roles in biology and immunopathology. Trends Mol Med. 2008 Oct 1;14(10):461–9.

16. Hara S, Kamei D, Sasaki Y, Tanemoto A, Nakatani Y, Murakami M. Prostaglandin E synthases: Understanding their pathophysiological roles through mouse genetic models. Biochimie. 2010;92:651–9.

17. Smith WL, Michael Garavito R, DeWitt DL. Prostaglandin endoperoxide H syntheses (cyclooxygenases)-1 and -2. J Biol Chem. 1996 Dec 27;271(52):33157–60.

bioRxiv preprint doi: https://doi.org/10.1101/2021.03.23.436585; this version posted March 23, 2021. The copyright holder for this preprint (which was not certified by peer review) is the author/funder, who has granted bioRxiv a license to display the preprint in perpetuity. It is made available under aCC-BY 4.0 International license.

711 18. Dubois RN, Abramson SB, Crofford L, Gupta RA, Simon LS, Van De Putte LBA, et al.
712 Cyclooxygenase in biology and disease. FASEB J. 1998;12:1063–73.
713 19. Hara S. Prostaglandin terminal synthases as novel therapeutic targets. Proc Japan Acad
714 Ser B, Phys Biol Sci. 2017;703–23.
715 20. Aoshi T, Carrero JA, Konjufca V, Koide Y, Unanue ER, Miller MJ. The cellular niche of
716 Listeria monocytogenes infection changes rapidly in the spleen. Eur J Immunol. 2009
717 Feb;39(2):417–25.
718 21. Noor S, Goldfine H, Tucker DE, Suram S, Lenz LL, Akira S, et al. Activation of
719 Cytosolic Phospholipase A 2 in Resident Peritoneal Macrophages by Listeria
720 monocytogenes Involves Listeriolysin O and TLR2 *. 2007;
721 22. Leslie CC. Cytosolic phospholipase A2: Physiological function and role in disease
722 [Internet]. Vol. 56, Journal of Lipid Research. American Society for Biochemistry and
723 Molecular Biology Inc.; 2015. p. 1386–402.
724 23. von Moltke J, Trinidad NJ, Moayeri M, Kintzer AF, Wang SB, van Rooijen N, et al.
725 Rapid induction of inflammatory lipid mediators by the inflammasome in vivo. Nature.
726 2012/08/21. 2012 Aug 19;490(7418):107–11.
727 24. Brockstedt DG, Giedlin MA, Leong ML, Bahjat KS, Gao Y, Luckett W, et al. Listeria-
728 based cancer vaccines that segregate immunogenicity from toxicity. Proc Natl Acad Sci U
729 S A. 2004 Sep 21;101(38):13832–7.
730 25. Kozak KR, Crews BC, Ray JL, Tai HH, Morrow JD, Marnett LJ. Metabolism of
731 Prostaglandin Glycerol Esters and Prostaglandin Ethanolamides in Vitro and in Vivo. J
732 Biol Chem. 2001 Oct 5;276(40):36993–8.
733 26. Abram CL, Roberge GL, Hu Y, Lowell CA. Comparative analysis of the efficiency and

bioRxiv preprint doi: https://doi.org/10.1101/2021.03.23.436585; this version posted March 23, 2021. The copyright holder for this preprint (which was not certified by peer review) is the author/funder, who has granted bioRxiv a license to display the preprint in perpetuity. It is made available under aCC-BY 4.0 International license.

specificity of myeloid-Cre deleting strains using ROSA-EYFP reporter mice. J Immunol Methods. 2014;408:89–100.

27. Pirgova G, Chauveau A, MacLean AJ, Cyster JG, Arnon TI. Marginal zone SIGN-R1+ macrophages are essential for the maturation of germinal center B cells in the spleen. Proc Natl Acad Sci U S A. 2020 Jun 2;117(22):12295–305.

28. van Rooijen N, Kors N, Kraal G. Macrophage subset repopulation in the spleen: differential kinetics after liposome-mediated elimination. J Leu. 1989;45(2):97–104.

29. Backer R, Schwandt T, Greuter M, Oosting M, Jüngerkes F, Tüting T, et al. Effective collaboration between marginal metallophilic macrophages and CD8 + dendritic cells in the generation of cytotoxic T cells. 2010;107(1):216–21.

30. Alzuguren P, Hervas-Stubbs S, Gonzalez-Aseguinolaza G, Poutou J, Fortes P, Mancheno U, et al. Transient depletion of specific immune cell populations to improve adenovirus-mediated transgene expression in the liver. Liver Int. 2014;

31. Crimmins GT, Herskovits AA, Rehder K, Sivick KE, Lauer P, Dubensky TW, et al. Listeria monocytogenes multidrug resistance transporters activate a cytosolic surveillance pathway of innate immunity. Proc Natl Acad Sci U S A. 2008 Jul 22;105(29):10191–6.

32. Huynh TAN, Woodward JJ. Too much of a good thing: Regulated depletion of c-di-AMP in the bacterial cytoplasm. Vol. 30, Current Opinion in Microbiology. Elsevier Ltd; 2016. p. 22–9.

33. McFarland AP, Luo S, Ahmed-Qadri F, Zuck M, Thayer EF, Goo YA, et al. Sensing of Bacterial Cyclic Dinucleotides by the Oxidoreductase RECON Promotes NF-κB Activation and Shapes a Proinflammatory Antibacterial State. Immunity. 2017 Mar 21;46(3):433–45.

bioRxiv preprint doi: https://doi.org/10.1101/2021.03.23.436585; this version posted March 23, 2021. The copyright holder for this preprint (which was not certified by peer review) is the author/funder, who has granted bioRxiv a license to display the preprint in perpetuity. It is made available under aCC-BY 4.0 International license.

34. Woodward JJ, Iavarone AT, Portnoy DA. c-di-AMP Secreted by Intracellular Listeria monocytogenes Activates a Host Type I Interferon Response. Science (80-). 2010 Jun 25;328(5986):1703–5.

35. Sauer J, Sotelo-Troha K, von Moltke J, Monroe KM, Rae CS, Brubaker SW, et al. The N-Ethyl-N-Nitrosourea-Induced Goldenticket Mouse Mutant Reveals an Essential Function of Sting in the In Vivo Interferon Response to Listeria monocytogenes and Cyclic Dinucleotides. Infect Immun. 2011 Feb 1;79(2):688–94.

36. Coulombe F, Jaworska J, Verway M, Tzelepis F, Massoud A, Gillard J, et al. Targeted prostaglandin E2 inhibition enhances antiviral immunity through induction of type I interferon and apoptosis in macrophages. Immunity. 2014/04/15. 2014 Apr 17;40(4):554–68.

37. Mayer-Barber KD, Andrade BB, Oland SD, Amaral EP, Barber DL, Gonzales J, et al. Host-directed therapy of tuberculosis based on interleukin-1 and type I interferon crosstalk. Nature. 2014 Jul 3;511(7507):99–103.

38. von Moltke J, Ayres JS, Kofoed EM, Chavarria-Smith J, Vance RE. Recognition of bacteria by inflammasomes. Annu Rev Immunol. 2012/12/12. 2013;31:73–106.

39. Martinon F, Mayor A, Tschopp J. The inflammasomes: guardians of the body. Annu Rev Immunol. 2009;27:229–65.

40. McDougal CE, Sauer JD. Listeria monocytogenes: The impact of cell death on infection and immunity [Internet]. Vol. 7, Pathogens. MDPI AG; 2018. p. 8.

41. Sauer J, Witte CE, Zemansky J, Hanson B, Lauer P, Portnoy DA. Listeria monocytogenes triggers AIM2-mediated pyroptosis upon infrequent bacteriolysis in the macrophage cytosol. Cell Host Microbe. 2010/04/27. 2010;7(5):412–9.

bioRxiv preprint doi: https://doi.org/10.1101/2021.03.23.436585; this version posted March 23, 2021. The copyright holder for this preprint (which was not certified by peer review) is the author/funder, who has granted bioRxiv a license to display the preprint in perpetuity. It is made available under aCC-BY 4.0 International license.

780 42. Hornung V, Ablasser A, Charrel-Dennis M, Bauernfeind F, Horvath G, Caffrey DR, et al.
781 AIM2 recognizes cytosolic dsDNA and forms a caspase-1-activating inflammasome with
782 ASC. Nature. 2009 Mar 26;458(7237):514–8.
783 43. Fernandes-Alnemri T, Yu J-WW, Datta P, Wu J, Alnemri ES. AIM2 activates the
784 inflammasome and cell death in response to cytoplasmic DNA. Nature. 2009 Mar
785 26;458(7237):509–13.
786 44. Martinon F, Burns K, Tschopp J. The inflammasome: a molecular platform triggering
787 activation of inflammatory caspases and processing of proIL-beta. Mol Cell. 2002/08/23.
788 2002 Aug;10(2):417–26.
789 45. Shi J, Zhao Y, Wang K, Shi X, Wang Y, Huang H, et al. Cleavage of GSDMD by
790 inflammatory caspases determines pyroptotic cell death. Nature. 2015 Sep
791 16;526(7575):660–5.
792 46. Kayagaki N, Stowe IB, Lee BL, O'Rourke K, Anderson K, Warming S, et al. Caspase-11
793 cleaves gasdermin D for non-canonical inflammasome signalling. Nature. 2015 Sep
794 16;526(7575):666–71.
795 47. Rauch I, Deets KA, Ji DX, von Moltke J, Tenthorey JL, Lee AY, et al. NAIP-NLRC4
796 Inflammasomes Coordinate Intestinal Epithelial Cell Expulsion with Eicosanoid and IL-
797 18 Release via Activation of Caspase-1 and -8. Immunity. 2017 Apr 18;46(4):649–59.
798 48. Glomski IJ, Decatur AL, Portnoy DA. Listeria monocytogenes mutants that fail to
799 compartmentalize listerolysin O activity are cytotoxic, avirulent, and unable to evade host
800 extracellular defenses. Infect Immun. 2003 Dec;71(12):6754–65.
801 49. Glomski IJ, Gedde M, Tsang A, Swanson J, Portnoy D. The Listeria monocytogenes
802 hemolysin has an acidic pH optimum to compartmentalize activity and prevent damage to

bioRxiv preprint doi: https://doi.org/10.1101/2021.03.23.436585; this version posted March 23, 2021. The copyright holder for this preprint (which was not certified by peer review) is the author/funder, who has granted bioRxiv a license to display the preprint in perpetuity. It is made available under aCC-BY 4.0 International license.

infected host cells. J Cell Biol. 2002/03/20. 2002 Mar 18;156(6):1029–38.

50. Schnupf P, Portnoy DA, Decatur AL. Phosphorylation, ubiquitination and degradation of listeriolysin O in mammalian cells: role of the PEST-like sequence. Cell Microbiol. 2006;8(2):353–64.

51. Nguyen BN, Portnoy DA. An Inducible Cre-lox System to Analyze the Role of LLO in Listeria monocytogenes Pathogenesis. Toxins (Basel). 2020 Jan 7;12(1).

52. Brock TG, Peters-Golden M. Activation and Regulation of Cellular Eicosanoid Biosynthesis. Sci World J. 2007;7:1273–84.

53. Tokudome S, Sano M, Shinmura K, Matsuhashi T, Morizane S, Moriyama H, et al. Glucocorticoid protects rodent hearts from ischemia/reperfusion injury by activating lipocalin-type prostaglandin D synthase-derived PGD2 biosynthesis. J Clin Invest. 2009 Jun 1;119(6):1477–88.

54. Biringer RG. The Enzymes of the Human Eicosanoid Pathway. Res Rep Med Sci. 2018;

55. Xiao L, Ornatowska M, Zhao G, Cao H, Yu R, Deng J, et al. Lipopolysaccharide-Induced Expression of Microsomal Prostaglandin E Synthase-1 Mediates Late-Phase PGE2 Production in Bone Marrow Derived Macrophages. Zhang L, editor. PLoS One. 2012 Nov 30;7(11):e50244.

56. Duncan KD, Fang R, Yuan J, Chu RK, Dey SK, Burnum-Johnson KE, et al. Quantitative Mass Spectrometry Imaging of Prostaglandins as Silver Ion Adducts with Nanospray Desorption Electrospray Ionization. Anal Chem. 2018 Jun 19;90(12):7246–52.

57. Markovič T, Jakopin Ž, Dolenc MS, Mlinarič-Raščan I. Structural features of subtype-selective EP receptor modulators. Vol. 22, Drug Discovery Today. Elsevier Ltd; 2017. p. 57–71.

bioRxiv preprint doi: https://doi.org/10.1101/2021.03.23.436585; this version posted March 23, 2021. The copyright holder for this preprint (which was not certified by peer review) is the author/funder, who has granted bioRxiv a license to display the preprint in perpetuity. It is made available under aCC-BY 4.0 International license.

826 58. Abramovitz M, Adam M, Boie Y, Carrière M-C, Denis D, Godbout C, et al. The
827 utilization of recombinant prostanoid receptors to determine the affinities and selectivities
828 of prostaglandins and related analogs. Biochim Biophys Acta - Mol Cell Biol Lipids. 2000
829 Jan 17;1483(2):285–93.
830 59. Krause P, Bruckner M, Uermö Si C, Singer E, Groettrup M, Legler DF. Prostaglandin E 2
831 enhances T-cell proliferation by inducing the costimulatory molecules OX40L, CD70, and
832 4-1BBL on dendritic cells. 2009;
833 60. Sheppe AEF, Kummari E, Walker A, Richards A, Hui WW, Lee JH, et al. PGE2
834 Augments Inflammasome Activation and M1 Polarization in Macrophages Infected With
835 Salmonella Typhimurium and Yersinia enterocolitica. Front Microbiol. 2018 Oct 31;9.
836 61. Mauel J, Ransijn A, Corradin SB, Buchmuller-Rouiller Y. Effect of PGE2 and of agents
837 that raise cAMP levels on macrophage activation induced by IFN-γ and TNF-α. J Leukoc
838 Biol. 1995;58(2):217–24.
839 62. Scandella E, Men Y, Gillessen S, Förster R, Groettrup M. Prostaglandin E2 is a key factor
840 for CCR7 surface expression and migration of monocyte-derived dendritic cells. Blood.
841 2002 Aug 15;100(4):1354–61.
842 63. Legler DF, Krause P, Scandella E, Singer E, Groettrup M. Prostaglandin E 2 Is Generally
843 Required for Human Dendritic Cell Migration and Exerts Its Effect via EP2 and EP4
844 Receptors . J Immunol. 2006 Jan 15;176(2):966–73.
845 64. Panzer U, Uguccioni M. Prostaglandin E 2 modulates the functional responsiveness of
846 human monocytes to chemokines.
847 65. Tajima T, Murata T, Aritake K, Urade Y, Hirai H, Nakamura M, et al. Lipopolysaccharide
848 induces macrophage migration via prostaglandin D 2 and prostaglandin E2. J Pharmacol

bioRxiv preprint doi: https://doi.org/10.1101/2021.03.23.436585; this version posted March 23, 2021. The copyright holder for this preprint (which was not certified by peer review) is the author/funder, who has granted bioRxiv a license to display the preprint in perpetuity. It is made available under aCC-BY 4.0 International license.

Exp Ther. 2008 Aug 1;326(2):493–501.

66. Yao C, Sakata D, Esaki Y, Li Y, Matsuoka T, Kuroiwa K, et al. Prostaglandin E 2-EP4 signaling promotes immune inflammation through T H 1 cell differentiation and T H 17 cell expansion. 2009;

67. Trebino CE, Stock JL, Gibbons CP, Naiman BM, Wachtmann TS, Umland JP, et al. Impaired inflammatory and pain responses in mice lacking an inducible prostaglandin E synthase. Proc Natl Acad Sci U S A. 2003 Jul 22;100(15):9044–9.

68. Nakanishi M, Montrose DC, Clark P, Nambiar PR, Belinsky GS, Claffey KP, et al. Genetic deletion of mPGES-1 suppresses intestinal tumorigenesis. Cancer Res. 2008 May 1;68(9):3251–9.

69. Nakanishi M, Menoret A, Tanaka T, Miyamoto S, Montrose DC, Vetta A, et al. Selective PGE 2 suppression inhibits colon carcinogenesis and modifies local mucosal immunity. Cancer Prev Res. 2011 Aug 1;4(8):1198–208.

70. Lutz MB, Kukutsch N, Ogilvie ALJ, Rößner S, Koch F, Romani N, et al. An advanced culture method for generating large quantities of highly pure dendritic cells from mouse bone marrow. J Immunol Methods. 1999 Feb 1;223(1):77–92.

71. Chen JH, Perry CJ, Tsui Y-C, Staron MM, Parish IA, Dominguez CX, et al. Prostaglandin E2 and programmed cell death 1 signaling coordinately impair CTL function and survival during chronic viral infection. Nat Med. 2015 Mar 23;21(4):327–34.

bioRxiv preprint doi: https://doi.org/10.1101/2021.03.23.436585; this version posted March 23, 2021. The copyright holder for this preprint (which was not certified by peer review) is the author/funder, who has granted bioRxiv a license to display the preprint in perpetuity. It is made available under aCC-BY 4.0 International license.

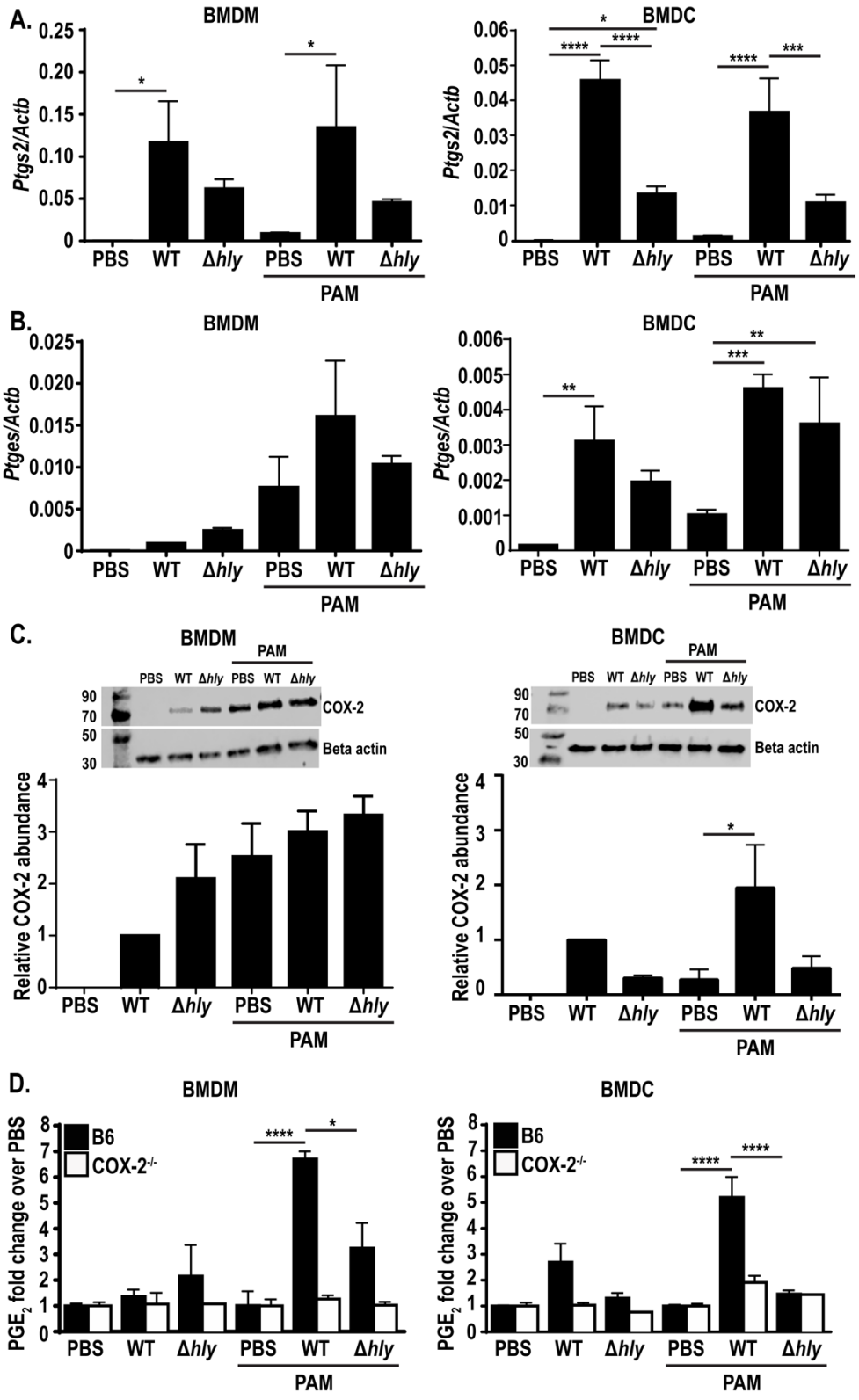

Fig 1

bioRxiv preprint doi: https://doi.org/10.1101/2021.03.23.436585; this version posted March 23, 2021. The copyright holder for this preprint (which was not certified by peer review) is the author/funder, who has granted bioRxiv a license to display the preprint in perpetuity. It is made available under aCC-BY 4.0 International license.

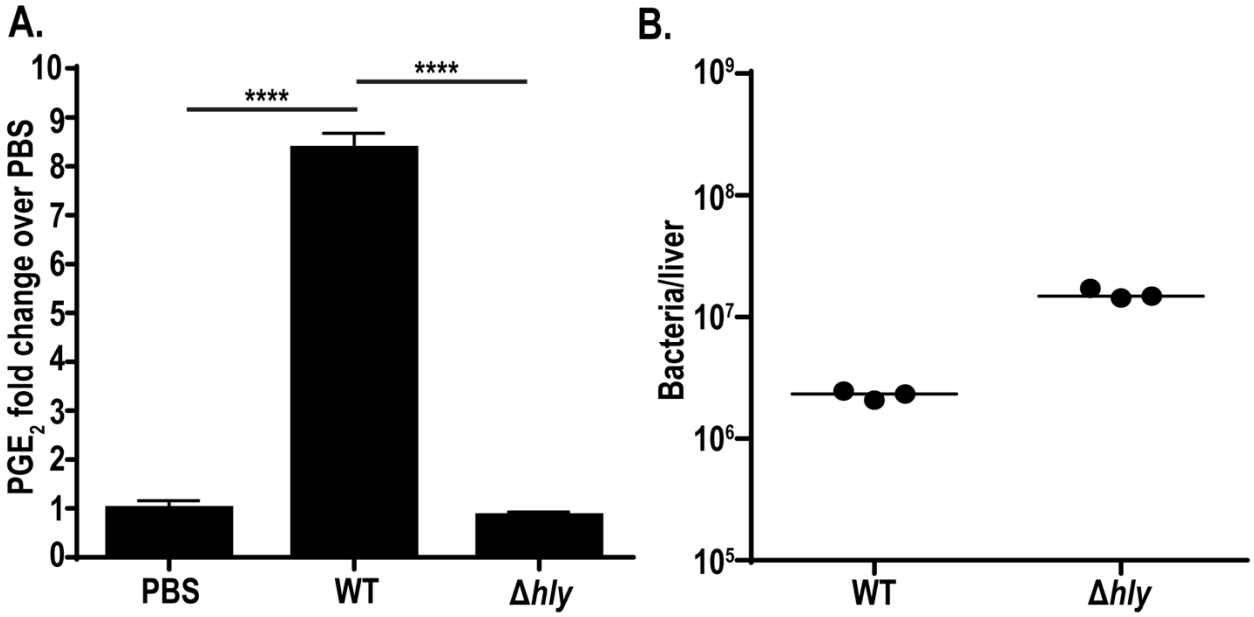

872

873 **Fig 2**

bioRxiv preprint doi: https://doi.org/10.1101/2021.03.23.436585; this version posted March 23, 2021. The copyright holder for this preprint (which was not certified by peer review) is the author/funder, who has granted bioRxiv a license to display the preprint in perpetuity. It is made available under aCC-BY 4.0 International license.

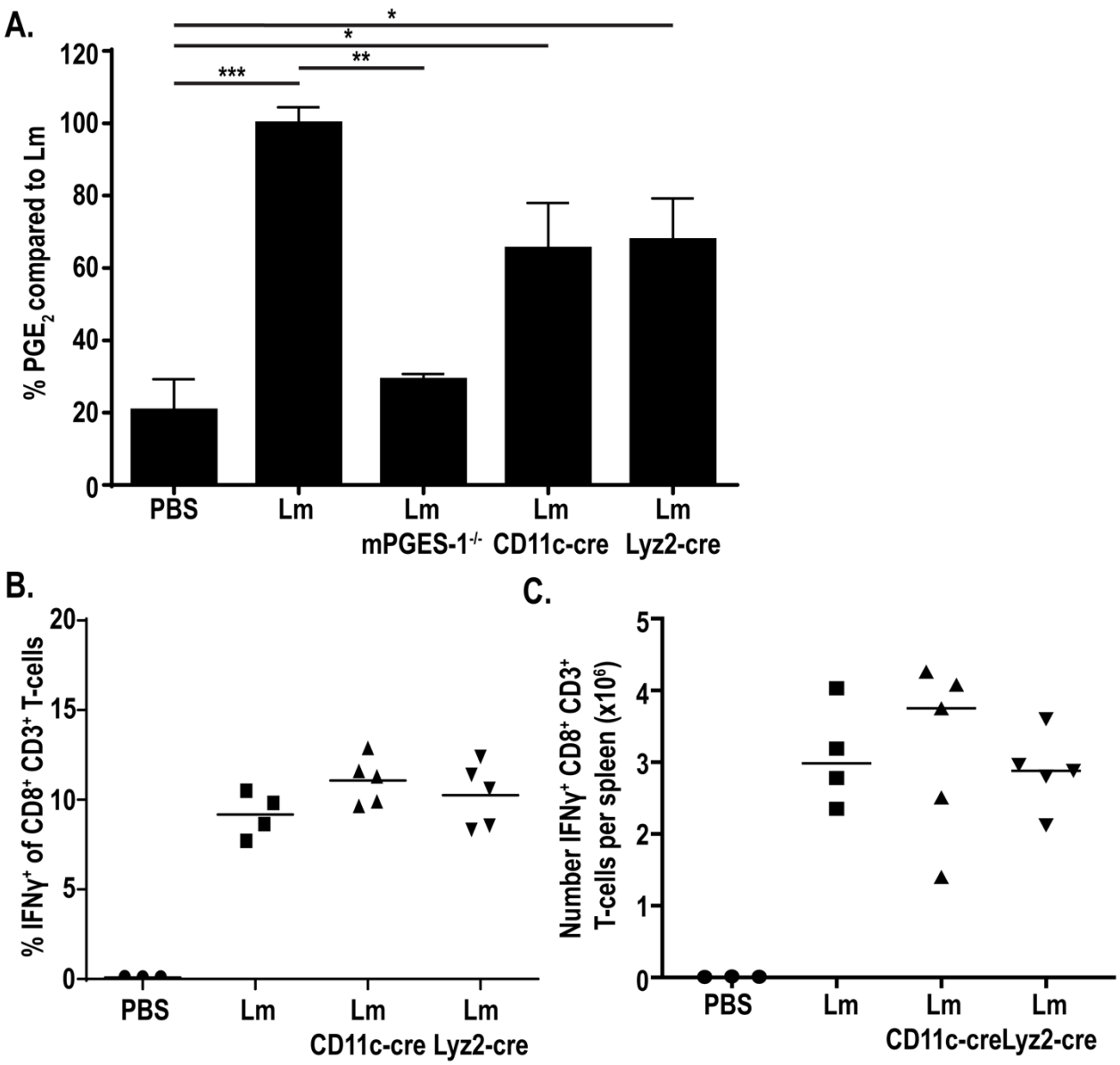

874

875 **Fig 3**

bioRxiv preprint doi: https://doi.org/10.1101/2021.03.23.436585; this version posted March 23, 2021. The copyright holder for this preprint (which was not certified by peer review) is the author/funder, who has granted bioRxiv a license to display the preprint in perpetuity. It is made available under aCC-BY 4.0 International license.

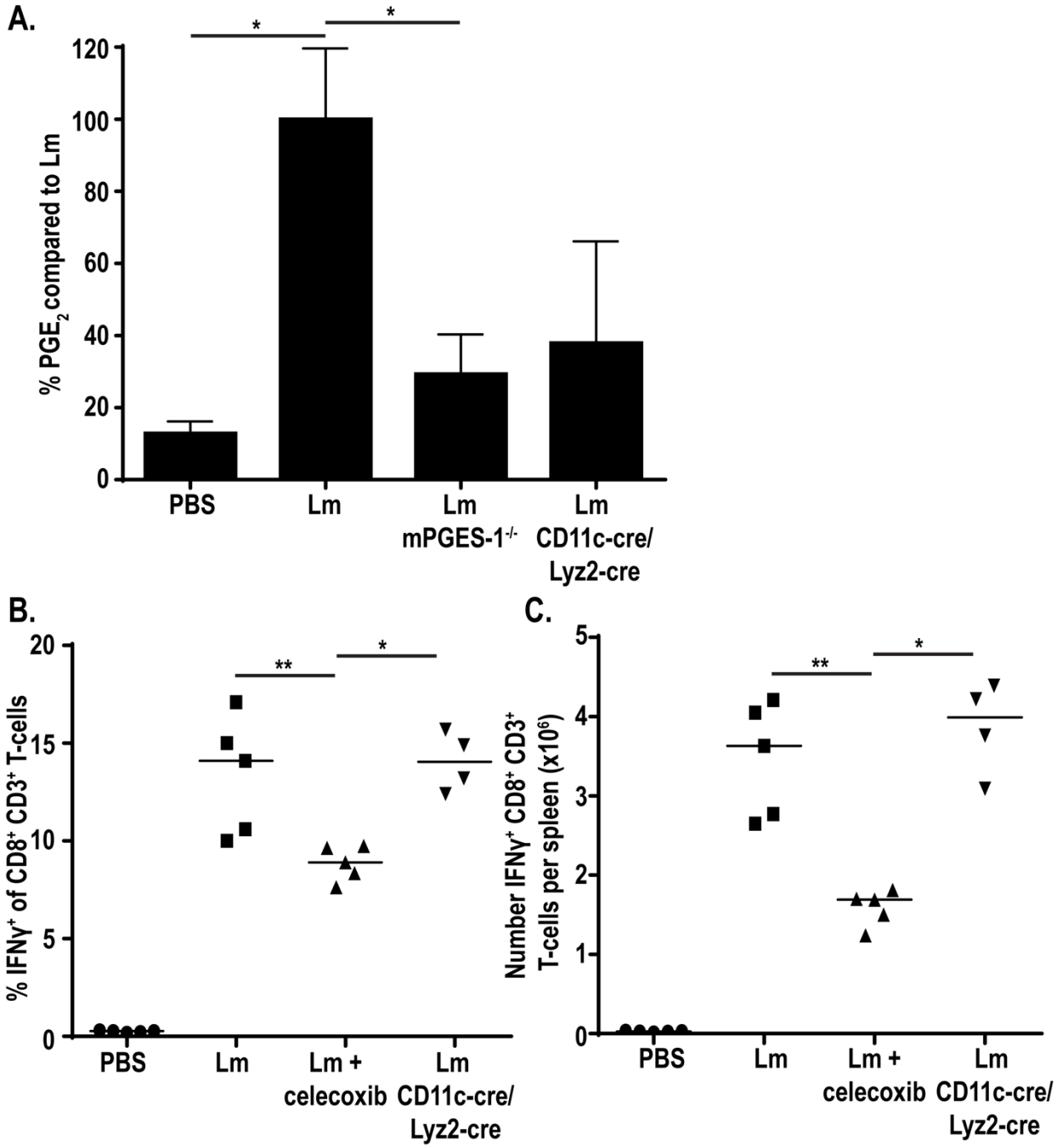

876

877 **Fig 4**

bioRxiv preprint doi: https://doi.org/10.1101/2021.03.23.436585; this version posted March 23, 2021. The copyright holder for this preprint (which was not certified by peer review) is the author/funder, who has granted bioRxiv a license to display the preprint in perpetuity. It is made available under aCC-BY 4.0 International license.

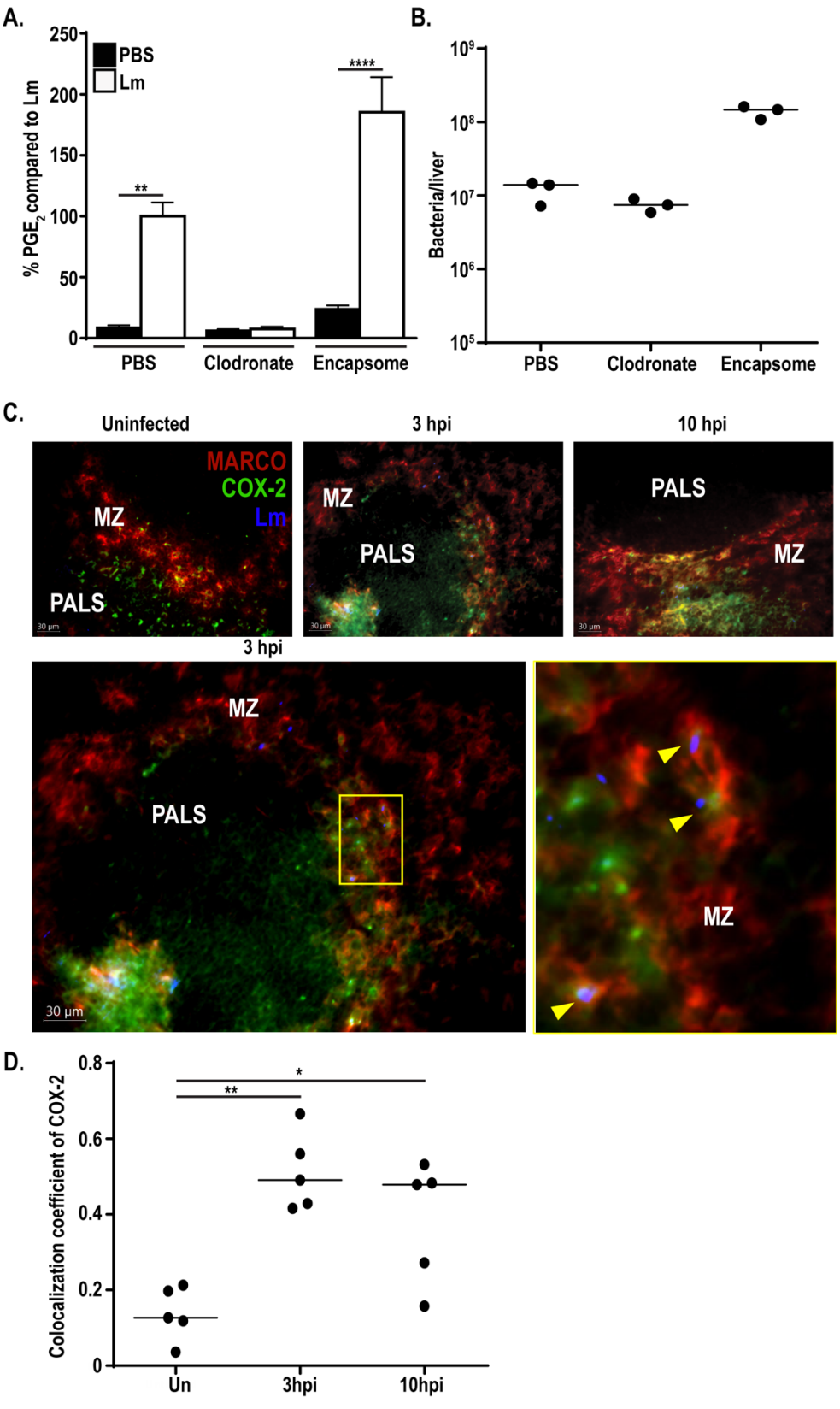

878

879 **Fig 5**

bioRxiv preprint doi: https://doi.org/10.1101/2021.03.23.436585; this version posted March 23, 2021. The copyright holder for this preprint (which was not certified by peer review) is the author/funder, who has granted bioRxiv a license to display the preprint in perpetuity. It is made available under aCC-BY 4.0 International license.

880 # Figure Legends

881 **Fig 1. PAM-primed BMDMs and BMDCs express PGE_2 after cytosolic infection with *L.***
882 ***monocytogenes*.** Wild-type or COX-$2^{-/-}$ BMDMs or BMDCs were infected with indicated strains
883 of *L. monocytogenes* at an MOI of 10 +/- the TLR2 agonist PAM3CSK4 and assessed 6hpi for
884 expression of *Ptgs2* (encoding COX-2) and *Ptges* (encoding mPGES-1) by qRT PCR (A-B) or
885 COX-2 protein by western blot (C). Supernatant was harvested and assessed for PGE_2 by mass
886 spectrometry (D). Mass spectrometry data was normalized to d-PGE_2 and fold change is relative
887 to PBS treated controls. Data are a combination of at least two independent experiments (A,B, D,
888 and western blot quantification), or a representative of at least two independent experiments
889 (western blot image). Significance was determined by a one-way ANOVA with Bonferroni's
890 correction. *$p < 0.05$, **$p < 0.01$, ***$p < 0.001$, ****$p < 0.0001$
891
892 **Fig 2. Cytosolic access is necessary for *L. monocytogenes*-stimulated PGE_2 production *in***
893 ***vivo*.** C57BL/6 mice were infected with 10^5 wild-type or 10^7 Δ*hly L. monocytogenes.* 12hpi
894 spleens were harvested for eicosanoid extraction and mass spectrometry (A) and livers were
895 harvested for bacterial burdens (B). Data are representative of two independent experiments.
896 Mass spectrometry data was normalized to d-PGE_2 levels and fold change is compared to PBS
897 controls. Significance was determined by a one-way ANOVA with Bonferroni's correction.
898 ****$p < 0.0001$
899
900 **Fig 3. $CD11c^+$ and $Lyz2^+$ cells contribute to PGE_2 production *in vivo*.** Indicated strains of
901 mice were infected with 10^7 LADD *L. monocytogenes*. 12hpi spleens were harvested and
902 assessed for PGE_2 by mass spectrometry. Data was normalized to d-PGE_2 levels and percent

bioRxiv preprint doi: https://doi.org/10.1101/2021.03.23.436585; this version posted March 23, 2021. The copyright holder for this preprint (which was not certified by peer review) is the author/funder, who has granted bioRxiv a license to display the preprint in perpetuity. It is made available under aCC-BY 4.0 International license.

903 change is compared to *L. monocytogenes*-infected controls (A). Indicated strains of mice were
904 infected with 10^7 LADD *L. monocytogenes*. 7dpi splenocytes were examined for B8R-specific
905 $CD8^+$ T-cell responses. %IFNγ (B) or number IFNγ (C) per spleen was assessed. Data shown are
906 representative of two independent experiments. Significance was determined by a one-way
907 ANOVA with Bonferroni's correction (A). *$p < 0.05$, **$p < 0.01$, ***$p < 0.001$
908
909 **Fig 4. Deletion of COX-2 in both $CD11c^+$ and $Lyz2^+$ cells further reduces PGE_2 production.**
910 Indicated strains of mice were infected with 10^7 LADD *L. monocytogenes*. 12hpi spleens were
911 harvested and assessed for PGE_2 by mass spectrometry. Data was normalized to d-PGE_2 levels
912 and percent change is compared to *L. monocytogenes*-infected controls (A). Indicated strains of
913 mice were infected with 10^7 LADD *L. monocytogenes*. 7dpi splenocytes were examined for
914 B8R-specific $CD8^+$ T-cell responses. %IFNγ (B) or number IFNγ (C) per spleen was assessed.
915 Data shown are representative of two independent experiments of 3-5 mice per group.
916 Significance was determined by a one-way ANOVA with Bonferroni's correction (A) or a
917 Mann-Whitney *U* test (B-C). *$p < 0.05$, **$p < 0.01$
918
919 **Fig 5. Phagocyte depletion eliminates PGE_2 production.** C57BL/6 mice were dosed with
920 200μL clodronate, liposome control (encapsome), or PBS 24 hours prior to immunization with
921 10^7 LADD *L. monocytogenes*. 12hpi spleens were harvested and assessed for PGE_2 by mass
922 spectrometry. Data was normalized to d-PGE_2 levels and percent change is compared to *L.*
923 *monocytogenes*-infected controls (A). Livers were harvested concurrently and assessed for
924 bacterial burdens (B). C57BL/6 mice were immunized with 10^7 LADD *L. monocytogenes.* 3 and
925 10hpi spleens were harvested, cryosections were cut, and sections were stained for *L.*

bioRxiv preprint doi: https://doi.org/10.1101/2021.03.23.436585; this version posted March 23, 2021. The copyright holder for this preprint (which was not certified by peer review) is the author/funder, who has granted bioRxiv a license to display the preprint in perpetuity. It is made available under aCC-BY 4.0 International license.

926 *monocytogenes* (Lm), COX-2, and MARCO (C). Yellow arrows represent colocalization of *L.*
927 *monocytogenes*, COX-2, and MARCO (C). Colocalization coefficients (Pearson's correlation) of
928 COX-2 and MARCO were calculated (D). Data shown are representative of at least two
929 independent experiments. Significance was determined by a one-way ANOVA with Bonferroni's
930 correction (A) or a Mann-Whitney *U* test (D). *$p < 0.05$, **$p < 0.01$, ****$p < 0.0001$